ELSEVIER

Coordination Chemistry Reviews
205 (2000) 157–199

COORDINATION CHEMISTRY REVIEWS

www.elsevier.com/locate/ccr

Cooperative binding in selective sensors, catalysts and actuators

Andrew Robertson, Seiji Shinkai *

Department of Chemistry and Biochemistry, Graduate School of Engineering, Kyushu University, Fukuoka 812-8581, Japan

Received 27 May 1999; accepted 31 December 1999

Contents

Abstract

This article is concerned with the incorporation of cooperative molecular recognition and metal ion coordination in the design of selective sensors that signal binding events through their optical properties. Sensors that rely on non-specific hydrophobic effects are first considered before looking at the use of specific, directed intermolecular interactions to achieve greater specificity and chiral discrimination. The natural development of the same

* Corresponding author. Tel.: +81-92-6423583; fax: +81-92-6324357.
E-mail address: seijitcm@mbox.nc.kyushu-u.ac.jp (S. Shinkai).

PII: S0010-8545(00)00243-5

design concepts to produce catalysts and actuating devices with similar discriminatory abilities is also discussed.

Keywords: Molecular-recognition; Sensor; Cooperativity; Allosterism; Catalysis; Selective

1. Introduction

1.1. The application of cooperativity

The need for materials with the ability to sense and report the presence of a desired chemical species is self-evident to scientists and engineers alike; correspondingly much research has been conducted to further their development. Molecules, or mixtures of molecules, that can report the presence of analytes through changes in optical properties [1] provide a particularly convenient means of detecting a sensing event — possibly the most familiar example of this kind of system is universal indicator, a mixture of pigments that allows simple determination of pH levels by a strong visible colour change. The use of spectrophotometry allows for a much more precise determination of changes in the absorption spectrum whilst simultaneously expanding the region of the spectrum that can be monitored. Other optical effects, such as changes in fluorescence intensity [2] afford further improvements in sensitivity and flexibility of sensor design.

Differentiation between similar analytes is much harder to achieve, however, small differences in chemical structure can make enormous differences in chemical action — one only needs to consider the variety of carbohydrates as a case in point. A sensor that can distinguish effectively between similar sugar structures, for example, would provide chemists and technologists with a very powerful tool for this area of research. An essential method for attaining high selectivities in chemical systems is to make use of two or more intermolecular interactions. This review therefore highlights examples of the use of cooperative binding effects that utilise metal ion coordination to bring about selectivity. The subject is further expanded to demonstrate the transfer of concepts that allow sensors to perform as catalysts and physical actions, as actuators, thereby coupling a molecule's ability to detect and report the conditions of its environment to an ability to change that environment. Molecules capable of sensing anions, however, are dealt with in a separate article within this issue and will not be specifically discussed here [3].

1.2. Sensors based on a single interaction

The field of simple, non-cooperative, metal-based receptors and sensors has been reviewed in a number of contexts [4,5] and will therefore only be exemplified briefly as an introduction to this topic. Most organic-based sensors make use of supramolecular host–guest interactions that promote only the discriminatory bind-

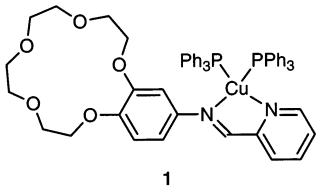

Fig. 1. A simple metal ion sensor. The crown ether complexes a simple cation thus changing the receptor's UV–VIS spectral properties.

ing of molecules with an appropriate arrangement of binding interactions. The basic concepts for sensors that make use of multiple interactions have been developed from relatively simple systems that use only one principal interaction. The copper-crown complex **1** produced by Yam and co-workers (Fig. 1) [6], for instance, relies on the well known affinity between a crown ether and alkali/alkaline earth cations for its sensing ability. Complexation with a suitable cation guest lowers the energy of the benzocrown low energy $\pi-\pi^*$ absorption band, which can be measured spectrophotometrically. Other sensors that rely on macrocycles to involve cations in a direct interaction with chromo/fluorophores include a similar design by Moore et al. [7], which uses a cyclam macrocycle connected to a ruthenium bipyridyl moiety and an azacrown–coumarin system reported by Valeur et al. [8].

A sensor that works as a result of a more dynamic interaction is depicted in Fig. 2 [9]. Pyrene and nitrobenzene moieties are appended to the lower rim of a calix[4]arene (**2**) through ester linkages which bring them into proximity, thus quenching fluorescence from the pyrene fluorophore by photoelectron transfer (PET) from its nitrobenzene counterpart. Metal binding to the pendant ester groups, however, induces a conformational change, which separates the aromatic moieties leading to a consequent increase in fluorescence.

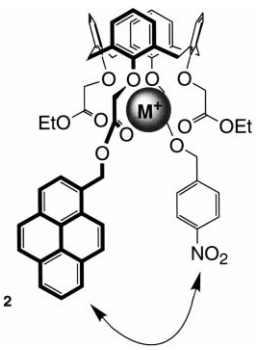

Fig. 2. Ion sensing by fluorescence enhancement. Metal coordination induces a rotation in the pendant esters, which separates the pyrene and nitrobenzene moieties thus increasing fluorescence.

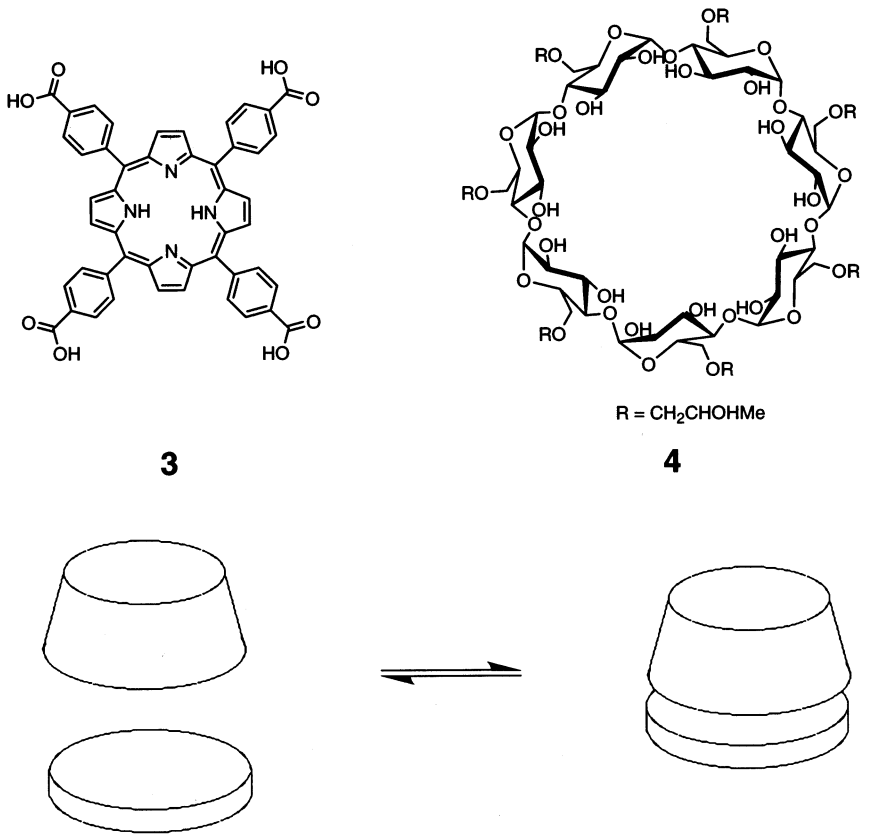

Fig. 3. A flat porphyrin and a conical cyclodextrin associate reversibly to form a cavity capable of discriminating between various substituted benzenes.

These sensors contain a basic recognition function that links metal coordination to a spectrophotometric function. Though simple in design, this very simplicity leads to difficulty in achieving efficient discrimination between cations with similar size and electronic properties. More complex interactions are required to achieve a good specificity, especially when organic molecules are the target analytes; in this case, a simple one-point interaction could lead to the recognition of many related compounds. An example of a slightly more complex system that does not involve metal coordination is illustrated in Fig. 3 [10] (**3**,**4**). This sensor links the ability of cyclodextrins to include hydrophobic molecules within its core to the spectral properties of a porphyrin to report on complexation. This molecule is therefore capable of selecting between various substituted benzenes and providing different signal responses.

2. Sensors that use cooperative binding

2.1. Introduction to cooperativity

Several binding interactions working in cooperation generate much greater flexibility and specificity in receptors [11,12] which, when coupled to a sensor function, allows for much greater discrimination between potential analytes. An example of the power that this approach affords can be seen in the bis-azacrown receptor for diammonium ions reported by de Silva and Sandanayake [13] (Fig. 4). The cooperative binding in this case allows for near atomic resolution of chain length with fluorescence as the signalling medium.

Cooperativity, therefore, enhances the function of sensors, for instance by changing a simple cation sensor into a sensor for a complete salt. Simultaneous binding of a cation and its associated anion naturally requires the use of a ditopic receptor with simultaneous electron donating and accepting ability — the inclusion of a suitable chromophore then transforms the receptor into a sensor. Porphyrins form a natural choice as the chromophore for the majority of these systems as metallated porphyrins provide a Lewis acid binding site for electron donors, whilst the extended π-system signals the occurrence of a binding event through its UV–VIS spectrum [14]. The use of circular dichromism (CD) spectroscopy [15,16] can provide further detail about the asymmetry of the host–guest complex [17], in some cases even providing absolute stereochemical information [18]. Furthermore, porphyrins make excellent platforms for functionalisation [19], can be highly symmetrical and are relatively straightforward to synthesise [20].

An example of these concepts is the receptor (**6**) illustrated in Fig. 5 [21], synthesised as the first example of a calix[4]arene capped porphyrin. As stated above, the metallated porphyrin is capable of binding to suitable anions whilst amide-appended calixarenes are known to be able to bind alkali cations thus providing a complementary cation binding site. The four-fold symmetry of the calixarene complements that of the porphyrin giving the whole molecule a C_4 symmetry whilst the chiral amino acids that form the four pendant 'pillars' render the molecule chiral overall.

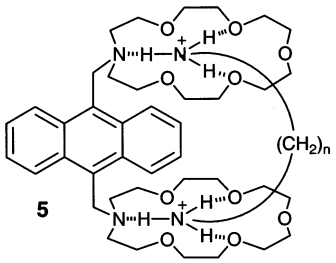

Fig. 4. Cooperative binding of a bis-ammonium dication coupled with preorganisation of the crown ethers allows for near atomic resolution of chain length.

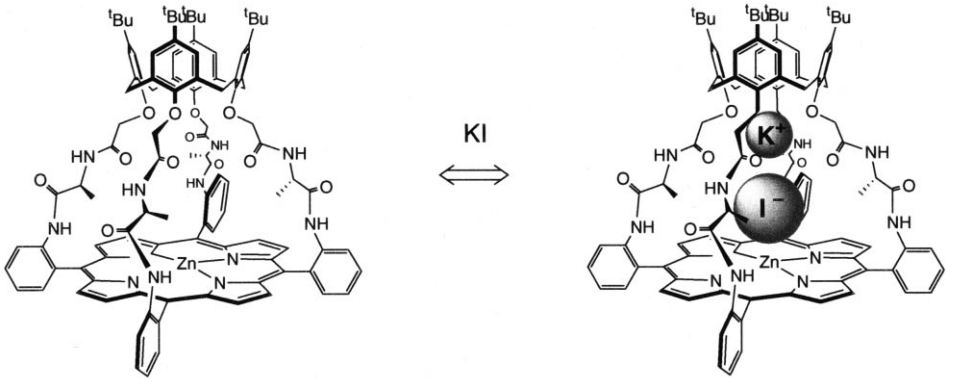

6

Fig. 5. A ditopic receptor for binary metal salts. The amide-appended calixarene can bind to cations whilst the metallated porphyrin can coordinate to anions. The ideal size of a potassium iodide ion pair allows the ions to interact with each other and with the receptor in a cooperative fashion.

Association constants in $CDCl_3$–MeCN could be estimated at around 10^3 M^{-1} for sodium and less than 10^2 M^{-1} for potassium and caesium. Lithium, however, showed differing binding constants of around 10^3 M^{-1} for the free base cavity and 10^5 M^{-1} for the zinc metallated cavity. The difference in behaviour between these alkali metal ions refers directly to the size of each salt. The small size of the lithium ion appears to allow it to exchange quickly on the NMR time scale whereas the larger ions exchange slowly. The larger potassium and caesium salts have binding constants that are too low to be measured by ^{1}H-NMR spectroscopic methods.

The nature of the anion also proved to be important in the ability of **6** to discriminate between different salts. The binding constants for $NaClO_4$ and NaI were of similar magnitude for the free-base **6** but NaI bound much more strongly to the zinc derivative of **6** than $NaClO_4$. Furthermore, KI and CsI were bound more strongly than NaI, in contrast to the perchlorate salts. This behaviour demonstrates that hole size is not the only factor in determining the binding strengths of salts to Zn–**6** but the positive role of the iodide anion must also be considered. The difference in behaviour between the perchlorate and iodide ions arises from the iodide ion's ability to coordinate directly to the central zinc ion, thus allowing Zn–**6** to actively bind to both parts of the salt as opposed to the cation-only binding mode of the free base **6**.

In the $NaClO_4$ case, the position of the UV–VIS maximum and the fluorescence maximum depend simply upon the concentration of the sodium ion because the perchlorate counter ion does not interact appreciably with the cavity. In the iodide case, at low concentrations, the complexation of the sodium cation is the predominant feature, comparable to the behaviour of $NaClO_4$. Upon increasing the concentration, complexation of the iodide counter-ion becomes important, shifting the Soret band with simultaneous fluorescence quenching. Unlike the sodium iodide

salt, in the potassium case, the potassium and iodide ions can interact simultaneously with both receptor sites and with each other. A similar non-metal system that senses ammonium fluoride using a crown ether-capped monoprotonated sapphyrin has also been reported by Sessler and Brucker [22].

These systems demonstrate the advantages of cooperative, ditopic binding. Individually, either receptor can bind cations or anions with modest selectivity. When incorporated into the same molecule, the complete salt can be accounted for, demonstrating that the application of a simple ionic sensor can thus be enhanced by the addition of a second, complementary interaction. An even more powerful application of the concepts of cooperative binding can be achieved by directing the combined power of the binding sites at one molecule or ion, for instance, the recognition of organic molecules and especially neutral molecules is strongly enhanced by the use of cooperative binding effects. Because this field is so vast, the sensors in this part of the review will be divided into recognition functions based on hydrophobic and steric interactions and those that are based on specific, directed, recognition functions.

2.2. Cooperativity through hydrophobic effects

A design based around cooperativity between a metallic Lewis acid, in this case zinc and hydrophobic effects, has been advanced by Imai and Kyuno (Fig. 6) [23], in the form of a 'picket fence' porphyrin.

This design was introduced as a model to mimic the hydrophobic pockets of heme proteins and thereby study the role of hydrophobic forces on substrate binding to these cavities. The restricted rotation of the phenyl groups generates four atropisomers [24], that can be thought of as being effectively non-interconvertible, though only the α^4 and *trans*-α^2 isomers are studied in this paper. The picket fence arrangement of peripheral substituents contributes steric buttressing and CH-π

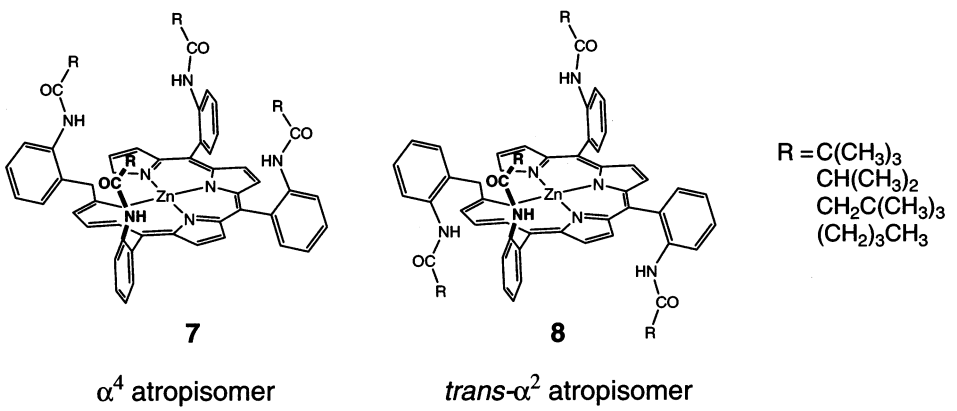

Fig. 6. A picket fence porphyrin, illustrating the α^4 atropisomer, hindered on one side only and the *trans*-α^2 atropisomer, hindered on both sides.

bonding to yield intermolecular forces complementary to the main nitrogen-zinc 'anchor'. They also define the spatial limits of the binding pocket.

By comparing the relative binding abilities of three nitrogen-donor bases: pyridine, isoquinoline and piperidine, to the iron-complexed porphyrin in non-polar solvents such as toluene and chloroform, the effect of the relative orientation of the pickets could be evaluated. It was found that the α^4 atropisomer directed binding predominantly towards the sterically free face, which could be expected in non-polar solvents. This allowed the α^4 porphyrin to be considered as a simple 'flat' porphyrin whilst still containing similar electronic and inductive effects to that of the *trans*-α^2 isomer. Different solvation abilities were expected to affect binding to the different atropisomers, however. Better solvation of the *trans*-α^2 atropisomer in toluene, as a result of the insertion of a molecule of toluene between the two co-facial pickets, was expected to reduce binding constants with this porphyrin whilst the crowded cavity of the α^4 atropisomer would remain vacant.

The most effective picket for base binding to the *trans*-α^2 isomer was found to be the pivalamido group. Although this group contains an amide with the least acidic NH proton in the study, Imai and co-workers [25] contend that it is relatively distant to the porphyrin plane, leading the authors to consider the difference in amide dipoles to be an unlikely candidate for the difference in binding abilities. The enhanced binding was ascribed, rather, to a difference in CH-π interactions. Indeed, the binding constants for pyridine and isoquinoline with the *trans*-α^2 isomer were similar to those for the α^4 isomer which can only accept binding to the 'free' face whilst the binding of isoquinoline was stronger for the *trans*-α^2 isomer where the π systems of the aromatic rings sit within the cavity formed by the 'picket fence'. Replacing the pivalamidopickets with structurally similar neopentyl pickets that could theoretically induce greater CH-π interactions resulted in a lower binding constant — this difference was attributed to the neopentyl chains being more flexible and therefore less pre-organised. The enhanced binding ability of the *trans*-α^2 isomer was not observed for the binding of piperidine, which does not contain a π system; in this case, steric repulsions appear to take a prominent position.

This study, though conceived as a model of enzymatic binding processes, demonstrates many important principles for designing selective sensors for organic molecules. Firstly, the coupling of a ligation site to steric buttressing groups creates a cavity that has specific affinities to molecules of a certain size and electronic nature. Secondly, the ligation site is also a chromophore, allowing for the detection of binding through spectrophotometric properties.

The logical progression from establishing separated blocking groups around the periphery of a porphyrin is to join those groups together to form 'straps' and 'caps'. The preceding 'picket fence' design was therefore adapted to include a bridge between co-facial ligands of a *trans*-α^2 atropisomer analogue [26] (Fig. 7) forming a 'double roofed porphyrin'.

The phenyl rings induce rigidity to aid preorganisation whilst the flexible linking chains define the limits of the cavity and prevent phenyl ring rotation. Compound **9** also has identical cavities on both sides in order to eliminate differences between

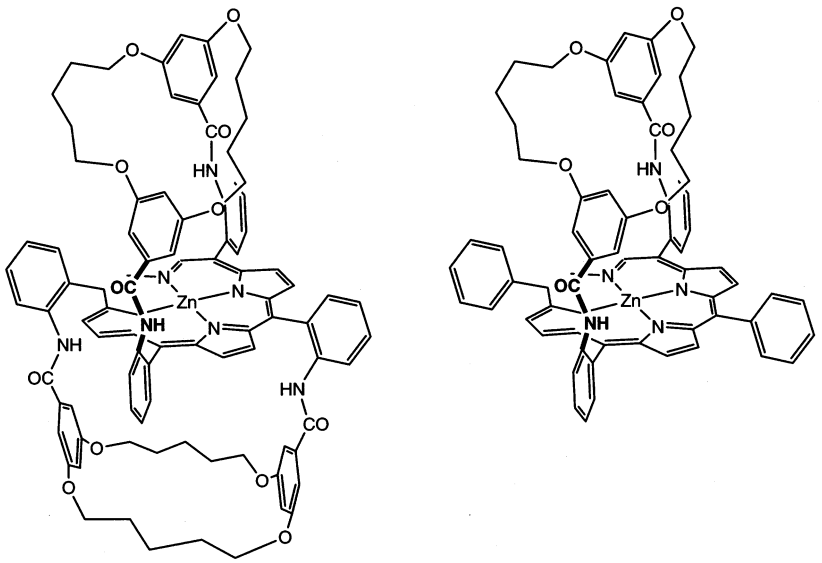

Fig. 7. A doubly and singly strapped porphyrin developed from a previous picket fence porphyrin (Fig. 6).

cavity binding and one-point 'free face' binding. Binding constants were measured by monitoring the change in the UV–VIS spectrum of **9** and all binding strengths were measured relative to that of butylamine. No difference in binding for any amines — whether primary alkyl, secondary alkyl or aromatic — was observed for the unconnected picket fence porphyrins, which is interesting given the results of the preceding paper. Although not explicitly stated, the picket fence porphyrin used for comparison was presumably the α^4 atropisomer as binding to the flat face was credited for the lack of selectivity.

Binding studies showed that the 'double-roofed porphyrin' was not very selective for primary amines. This lack of discrimination presumably arises because the aliphatic portions can point out of the cavity and are therefore not sufficiently constricted to be forced to interact with the straps. The secondary aliphatic amines, however, showed very different abilities to ligate the central zinc atom. Selectivity was greatest for small, cyclic ligands such as azetidine, diethylamine and pyrrolidine; following on were the large acyclic aliphatic ligands and finally large cyclic ligands, which showed no particular selectivity at all. This behaviour has been attributed to two different interactions between the cavity and the ligands. One interaction involves the aliphatic side-chains sitting snugly inside the cavity; this is the predicted binding mode of the smaller secondary amines and yields the greatest selectivity because positive, attractive van der Waals forces quickly give way to steric repulsion as the size of the ligand increases. The other main binding mode

requires a sterically bulky ligand to push the strap aside to allow binding. This is the favoured binding mode of the large cyclic amines but does not allow for any selectivity. The acyclic binding mode is constricted to the first, 'inside cavity' case, however, as a result of the larger C–N–C bond angle, which results in good selectivity on increasing ligand size.

The aromatic amines, however, did not appear to display any form of selectivity, which was surprising considering that an additional π–π interaction should be available to aid discrimination. It is postulated that attractive and repulsive forces balance each other for these compounds, though the authors concede that there are probably other factors to be considered.

This paper concludes by suggesting that there is an ideal fit that maximises the stability of each complex. An ideal ligand will be small enough to fit into the cavity without any steric repulsions whilst large enough to maximise attractive van der Waals forces. The combination of these factors generates selectivity. Upon cleaving the restraining links between the pendant phenyl groups [27], selectivity was observed to decrease dramatically, demonstrating the need for some form of preorganisation for obtaining selectivity.

Capped porphyrins provide even more constrained cavities [28] with possible applications as heme analogues [29] in addition to sensing applications. Using concepts similar to those for designing the potassium iodide sensor [20] described above (Fig. 5), a calixarene-capped porphyrin **11** was able to make use of cooperative binding to enhance binding to a cationic derivative of isoleucine [30] (Fig. 8).

Through cation-π binding effects, additional to the main Zn–N ligation, an increase in binding enthalpy of around 20% for the cationic ligand, versus it's neutral equivalent, was observed.

An interesting study by Diederich and co-workers [31] demonstrated that a guest can be induced to form a UV active complex within a cavity, even when it has the

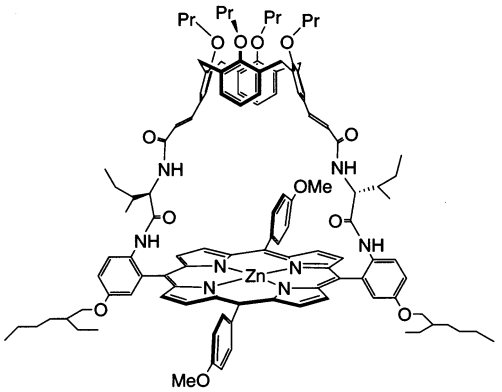

11

Fig. 8. A capped porphyrin capable of discriminating between amino acids.

choice between binding inside and outside. In this case, two versions of a capped porphyrin were synthesised, one singly strapped, **12**, and one doubly strapped, **13**, (Fig. 9).

These hosts were unable to complex simple aromatic molecules such as benzene and naphthalene but could bind effectively to pyridine which can coordinate to the Zn ion through strong Zn–N binding. This behaviour was accredited to the lack of preorganisation of the binding site; the entropic penalty of organising the caps is compensated for by the enthalpic bonus from Zn–N ligation for pyridine-type molecules but no such compensation is available to non-donating molecules. An extra factor in these studies is that of solvent effects; the studies were performed in methanol, which is a weak competitor for the zinc binding site but present in a much greater concentration, which should greatly reduce pyridine binding. Although the poor solubility of tetraphenylporphyrin prevented a direct comparison, 3,5-lutidene, a molecule too large to fit within the cavity, did not bind significantly to **13**. Furthermore, the binding constants for pyridine binding to **12** and **13** were similar in both cases and similar complexation-induced shifts were observed by ^{1}H-NMR spectroscopy. The conclusion drawn from these experiments, therefore, is that when given the choice between binding within the cavity or on the exposed face

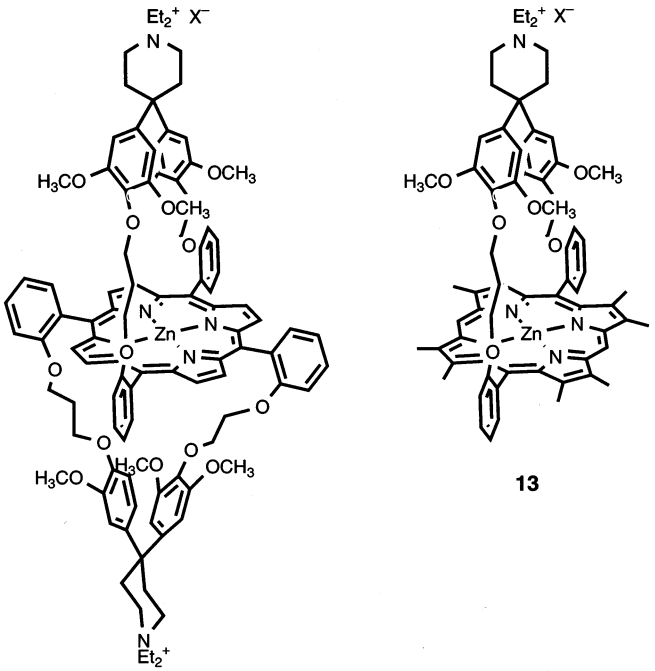

Fig. 9. A doubly-strapped porphyrin capable of binding aromatic *N*-donor ligands. Complexation occurred within the cavity even when a free face was made available by appending only one strap.

of **12**, the N-donor ligands prefer the cavity, which is solvent free. When all of these properties are taken together, it can be seen that a flexibly capped porphyrin can function as a UV-active receptor with the ability to discriminate in favour of molecules that have both the correct donor ability and the correct size.

Cyclodextrin-capped porphyrins can make use of highly preorganised cavities. One example of a doubly capped porphyrin **14** (Fig. 10), reported by Kuroda et al. [32], can signal four different binding states through its UV–VIS spectrum. The iron(III) complex of this capped porphyrin gives distinctly different UV–VIS spectra between empty cyclodextrins, a single benzylmercaptan complexed species, the doubly occupied benzylmercaptan species and the benzyl mercaptan/1-adamantanecarboxylate heterocomplex.

Using inclusion effects with porphyrin systems took a novel direction with the construction of a self-assembling porphyrin dimer [33]. Peripheral benzyl carboxylic acids promote self-association of the α^4 atropisomer in chloroform to form a cavity composed of the two porphyrins (Fig. 11).

Evidence for the formation of the dimer in non-polar solvents was obtained from vapour pressure osmometry and by comparison of the UV–VIS spectrum in dichloromethane and tetrahydrofuran. The bidentate ligand pyrazine was found to bind to the zinc-metallated porphyrin dimer in a porphyrin–pyrazine ratio of 2:1 with a binding constant in CH_2Cl_2 that was too high to measure and so could only be estimated as being higher than 10^7 M^{-1}. Monodentate and large bidentate ligands however show no appreciable complex formation at low concentrations of less than 5×10^{-5} M, though 1:1 complexes were formed at higher concentrations. This experiment demonstrated the concept of a self-assembling UV-active cavity capable of ligand donor and shape discrimination. An interesting development was the observation that pyrazine derivatives with bulky side chains could ligate inside the cavity with the side chain 'sticking out' of the side. This raises the possibility of a UV active sensor that can bind to selected portions of a molecule that would otherwise be too large to fit inside.

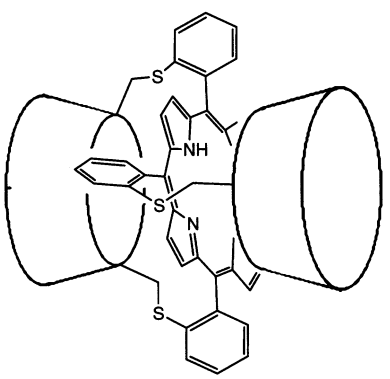

14

Fig. 10. Doubly-strapped porphyrin capable of sensing four different binding conditions.

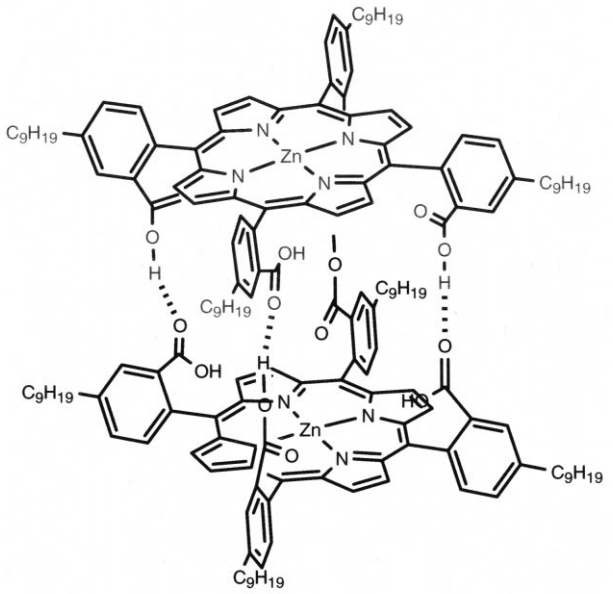

15

Fig. 11. Intermolecular hydrogen bonds between pendant carboxylic acids promote dimer formation of this porphyrin creating a cavity suitable for inclusion of suitable guests. Bulky side-chains of included compounds can protrude from the four orifices framed by the four hydrogen bonding interactions.

2.3. Cooperativity through specific interactions

An approach that brings together the principles of cavity-based hydrophobic interactions and directed hydrogen bonding interactions has been advanced by Bonar-Law and Sanders [34]. In this design, a capped porphyrin was formed from cholic acid and a zinc-metallated porphyrin (**16**) forming a cup-shaped cavity with convergent alcohol moieties (Fig. 12).

Binding studies between the steroidal 'roof' (**17**) and various diols revealed weak, unselective interactions, whereas selected pyranosides demonstrated an ability to form discrete 1:1 complexes as well as 2:1 complexes where a single pyranoside is sandwiched between two cholesterol units. This demonstrated the convergent and cavity forming properties of the steroidal 'roof'.

The binding of methanol to **16** revealed some interesting cooperative behaviour for this small alcohol through UV–VIS spectra. The first binding event was unremarkable but a second binding event resulted in greater stability (5.7 kJ mol^{-1}, relative to the control) as a result of the second molecule forming a hydrogen bonded bridge between the Zn-coordinated methanol and the steroidal cap (Fig. 13)

These properties allowed the capped porphyrin to show a modest selectivity on recognition of the pyranosides mannose, glucose and galactose with complex

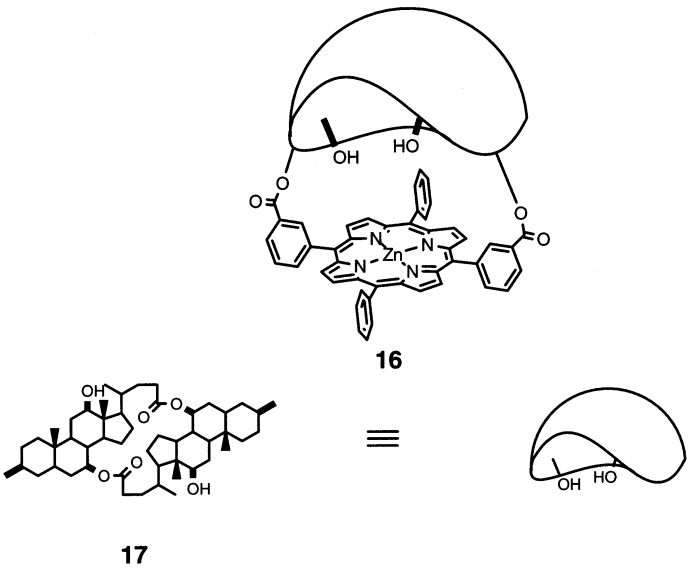

Fig. 12. Cholesterol capped porphyrin. This design combines the concept of a simple cap with that of directional hydrogen bonding interactions.

stability decreasing in that order. The presence of the Zn-metallated porphyrin led to a distinct colour change of the solution from pink to yellow–green upon complexation thus allowing convenient analysis by UV–VIS spectroscopy. The shifts in the Soret band were similar to those obtained for strongly bound alcohols and so it appears that the sugars bond directly to the central zinc atom.

The selectivity, however, was not attributed to discrete hydrogen-bonding interactions but rather to the inherent freedom of the pyranosides to bind to other molecules. Further thermodynamic studies involving low concentrations of methanol and water in non-polar solvents revealed some very interesting facts. Rather than competing directly for the hydrogen bonding sites within the receptor, the small polar molecules co-operate with the pyranoside to make a hydrogen-bonded chain and actually increase the overall stability of the complex. The authors

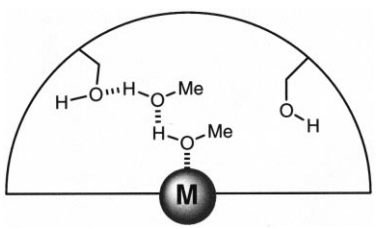

Fig. 13. Methanol molecules bind co-operatively to enhance binding and create a bridge between the central zinc ion and one of the cap hydroxyls.

suggest that these effects could be used to enhance the binding ability of an otherwise poor-fitting guest. This behaviour is naturally a two-edged sword as it increases the flexibility of a preorganised receptor whilst simultaneously reducing its selectivity. The studies in this paper highlight the importance of a number of small but intricate processes that form an essential part of ligand binding in polar solvents.

The authors conclude that this does not change the fact that α-mannoside binds more strongly to the receptor than β-galactoside but it does mean that a simpler receptor cavity could probably perform the same task. Furthermore, it was discovered that the free base receptors could bind pyranosides almost as well as the Zn-metallated version. Computer modelling suggested that the pyranosides were not bulky enough to occupy the full cavity of the receptor and were rather adhering predominantly to the 'roof'. Weakly cooperative three point binding modes to the cap hydroxy functions resulted in the enhanced binding within the receptor, as opposed to a strong Zn–O bond.

A very simple example [35] of directionality-controlled cooperative binding involves the study of Zn-metallated gable porphyrins (Fig. 14). In this case, the convergent arrangement of the porphyrin gable allows cooperative binding of diamines through simultaneous binding to the *endo* face of the porphyrin dimer. When binding to the monometallated gable porphyrin, the diamines showed behaviour very similar to that observed when binding to a simple tetraphenyl porphyrin with binding predominantly on the less hindered *exo* face. When binding to the bismetallated gable porphyrin, the diamines coordinate to the more hindered *endo* face but with a much higher binding constant.

The use of hydrogen bonding sites incorporates directionality into the recognition process. Amino acids are particularly suitable candidates for cooperative binding

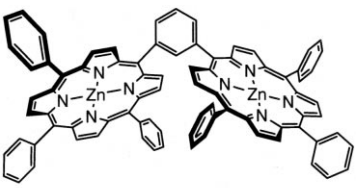

18

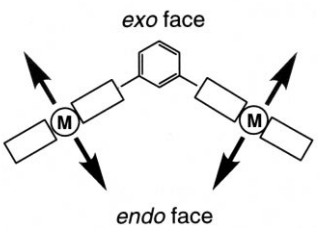

Fig. 14. A gable porphyrin capable of either convergent or divergent binding.

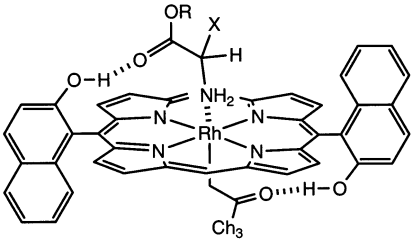

19

Fig. 15. Cooperativity between a Rh–N interaction and a carbonyl–hydroxyl interaction enhances differentiation between different amino acids.

between a metal coordination site and a hydrogen bond donor as a result of the electron donor ability of the amine function and hydrogen-bond acceptor role of the carbonyl group [36]. Ogoshi et al. [37] have commented on the importance of bifunctional porphyrins for probing subtle hydrogen bonding interactions as a result of their sensitivity to UV–VIS spectroscopy; an example of this kind of cooperativity is presented in Fig. 15.

The most important coordination is attained through strong Rh–N binding with secondary interactions between the ester carbonyl function of the amino acid and the hydroxyl group of the hydroxynaphthyl moiety attached to the Rh-metallated porphyrin. The overall binding was very strong with no observable dissociation of any adducts after HPLC. This binding is, however, too strong to be of use for selectivity or sensing and so the more labile Zn-metallated derivative was used. The fast exchange between ligands permitted the *trans*-OH atropisomer of **19** to form a complex with L-leucine methyl ester in a 20-fold excess over 4-amino heptane when these components were mixed in a ratio of 1:2:2 of porphyrin to amines, respectively.

Ogoshi et al. [38] continued the theme of this research by including an ester group on the periphery of the porphyrin to act as a steric barrier. The use of three separate binding interactions was intended to provide a means of chiral discrimination as the *trans*-OH atropisomer of **20** presents a chiral array of interaction sites (Fig. 16).

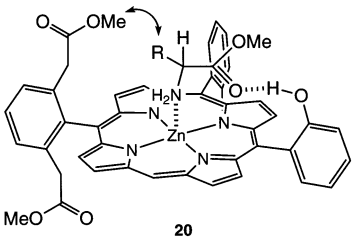

20

Fig. 16. A three-point interaction between a porphyrin and an amino acid. In addition to the N–Zn and hydrogen bonding attractions, a methyl ester acts as a steric repulsion unit. The *trans*-OH atropisomer is shown here.

Naturally, the binding of the receptor and associated model compounds could be followed by UV–Vis spectroscopy, thus allowing a convenient determination of binding constants. The methyl ester group of the (+)-enantiomer was found to take part in three separate interactions depending on the nature of the guest: a minor steric blocking force for L-amino acid esters; a major steric blocking force for D-amino acid esters and an attractive force for D-Ser-OBzl.

The hydrogen-bonding interactions exhibited a mild preference for L-amino acids with free energies of binding in the region of -1.1 to -1.3 kcal mol^{-1} for the L-amino acids and -0.6 to $+0.8$ kcal mol^{-1} for the D-amino acids. The steric repulsion for the L-amino acids was found, by model studies, to be similar for both the one-point, Zn–N linked adducts and for the two-point, Zn–N/H-bond linked adducts. In the case of the D-amino acids, however, forming the two-point adduct actually increases the steric repulsion penalty, thus generating cooperativity between the hydrogen bonding sites, that preferentially attract L-amino acids and the steric blocking group that preferentially repels D-amino acids.

The apparent discontinuity for D-Ser-OBzl was tentatively attributed to the formation of a hydrogen bond between the side-chain hydroxy group of D-Ser-OBzl and the carbonyl function of the porphyrin methyl ester with a stabilisation energy in the region of -0.6 to -1.1 kcal mol^{-1}, based on the sum of apparent stabilising energy and steric repulsion energy for other D-amino acids. The attractive interaction for D-Ser-OBzl results in a reversal of enantioselectivities for this amino acid — the ester blocking function was found to act as a steric repulsion factor for the 'misfit' L-Ser-OBzl.

These practical observations were later developed into interesting theoretical studies on multiple site interactions between amino acids and porphyrins that drew a number of conclusions pertinent to the design of sensors [39]. The advantages of multiple binding sites using cooperative binding were cited as allowing stronger association through fast association without hindering the dissociation process, an important factor also for high turnover in catalytic systems. They also reported a method for quantifying the internal rotation of potential guests/analytes, which allows for better estimations of binding affinities [40].

An interesting system produced by Maverick et al. [41] uses metal coordination simultaneously for assembling the receptor and as the guest binding sites (Fig. 17).

The two copper centres allow cooperative inclusion of small nitrogenous bidentate bases. It was noted that olive-green solutions of receptor **21** turned to a turquoise colour upon addition of nitrogenous bases. Though pyrazine itself was capable of binding effectively within the cavity, the substituted pyrazines were found to be less stable. The 2-aminopyrazine derivative, however, displayed stronger binding as a result of additional hydrogen bonding between an amine proton and one of the diketone carbonyl moieties.

Another example that uses metal coordination to assemble a receptor for cooperative binding has been reported by Hamilton and co-workers [42]. A phenanthroline-based ligand coordinates to a copper(I) ion to assemble two amidopicoline groups into a tweezer arrangement suitable for binding dicarboxylic acids (Fig. 18).

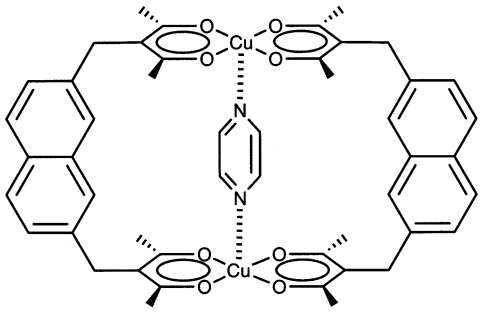

21

Fig. 17. A self-assembling cavity that coordinates to nitrogenous bases through cooperative binding.

The phenanthroline moieties also act as convenient spectroscopically active functions for reporting binding events. Binding constants in $CHCl_3$ for a number of related dicarboxylic acids were determined spectroscopically to be in the order of 1.5 to 7.0×10^4 M^{-1} and a slight colour change from red to orange–red was observed upon binding which was highly sensitive to the chain length of dicarboxylic acids. The chiral nature of **22** was noted and, indeed, diastereomeric signals were observed by ^{1}H-NMR spectroscopy upon addition of *N*-Cbz-L-glutamic acid to a racemic mixture of the receptor, though there was no observable selectivity.

The design was improved by appending the acid tweezers to both ends of the receptor [43]. In this case, the colour changes were more noticeable but with binding constants similar to those for **22** (1.7 to 7.8×10^4 M^{-1}). The origin of the colour change could not be properly determined, though it was directly attributable to coordination of the dicarboxylic acids and, more specifically, to a change in geometry of the receptor upon acid recognition. This study demonstrates the self-assembly of a chiral, chromogenic receptor from achiral building blocks that makes use of cooperative hydrogen bonding effects to attain specificity.

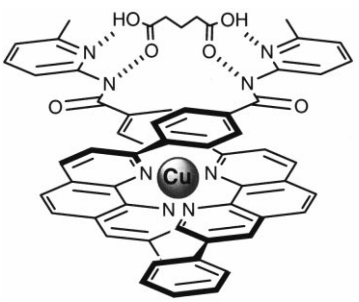

22

Fig. 18. Assembly of the two phenanthroline 'arms' around a copper ion brings two amidopicoline moieties into a suitable configuration for binding dicarboxylic acids.

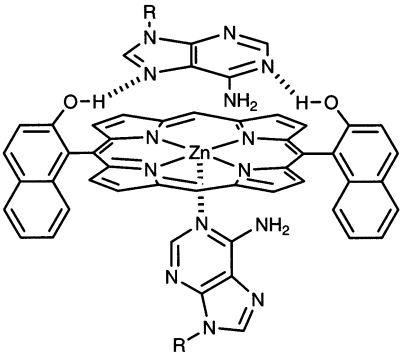

23

Fig. 19. Binding of adenine in the plane of the porphyrin using cooperative hydrogen bonding attractions whilst allowing simultaneous binding to the central Zn ion from the opposite side.

An alternative binding orientation for a simple nucleobase has also been studied [44]. In this design, one molecule of adenine is held in an orientation parallel to the porphyrin ring plane through cooperative hydrogen bonds whilst another molecule can simultaneously coordinate to the central Zn atom (Fig. 19).

The 2:1 binding mode was confirmed by UV-titration experiments and ^{1}H-NMR spectroscopy studies suggested that formation of the hydrogen bonding mode is the first step of the binding process. This design was later developed to function in a similar manner for quinone binding (Fig. 20) [45].

A departure from the more common parallel orientation of H-bond and porphyrin planes was advanced by Chang and co-workers [46]. This arrangement uses a 'hanging' hydrogen-bond donor in the form of a pendant Kemp's triacid to bind dioxygen as it simultaneously coordinates to a central Co(II) ion in a 'C-clamp'

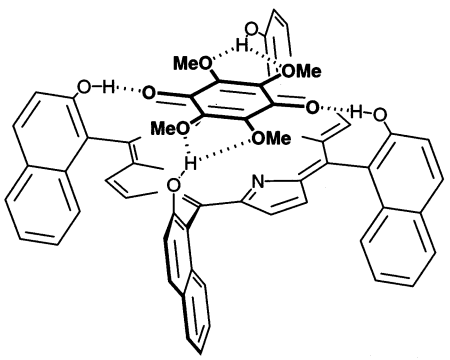

24

Fig. 20. In-plane binding of a quinone derivative through multi-point binding.

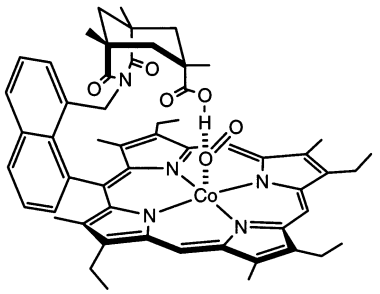

25

Fig. 21. A hanging 'C-clamp' binding motif, able to pin an oxygen molecule between the Co atom and the suspended hydroxyl hydrogen.

array (Fig. 21). The advantage that this arrangement has over the traditional orientation of H-bond donors is that, in this case, the hydrogen bond is directed at the cobalt-coordinated oxygen atom. Although this hydrogen bond is not as strong as one directed at the 'free' oxygen atom, the oxygen molecule retains more entropic freedom with a corresponding reduction in the entropic penalty for binding. This is an important concept for sensors which require fast exchange whilst maintaining overall binding ability because this design does not require high binding enthalpies that can lead to slow exchange.

The same concept was modified by replacing the naphthyl spacer with anthracene to allow selective binding of small heteronuclear bases with binding detectable by UV–Vis spectroscopy [47]. Small bases such as imidazole and purine bound to the anthracene derivative with similar binding constants in $CHCl_3$ of around 2.6×10^3 M^{-1} demonstrating that bascicity was not a factor in binding strength. Triazole, however, normally a weak ligand for Zn-metallated porphyrins with a binding constant for Zn-octaethyl porphyrin of around 3.9×10^2 M^{-1}, was able to bind with an association constant of around 1.8×10^4 M^{-1} as the result of a combination of cooperative hydrogen bonding and Zn–N ligation.

2.4. Using cooperative binding to create chirally selective sensors

A very important property of UV active receptors is their ability to shed light on achiral complexes through the use of circular dichromism spectroscopy [15]. This method essentially uses a through space interaction between two chromophores to obtain a spectrum for asymmetric compounds and, in some cases, to determine the absolute chirality of that species. Linking a UV active receptor to a chiral guest provides a powerful method for generating chirality sensors — including cooperative associations into the receptor generates a selective chirality sensor.

A simple design of this kind [48] involves the recognition of uronic acids and sialic acids by linking a phenanthroline chromophore to a boronic acid primary recognition site (Fig. 22). The phenanthroline moiety is a fluorophore but pho-

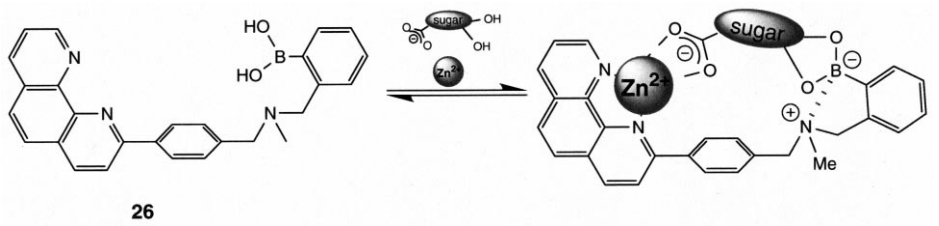

Fig. 22. A phenanthroline–boronic acid coupled system — cooperative binding of uronic acids is achieved through simultaneous boronic ester formation and Zn ion complexation.

toelectron transfer (PET) from the tertiary amine quenches the fluorescence in the free state. Saccharide recognition at the boronic acid site, however, ties up the nitrogen lone pair in a N–B dative bond, thus resulting in an increase of fluorescence upon saccharide binding. Titration of the neutral receptor with various saccharides in MeOH–H_2O demonstrates an increase in fluorescence with moderate selectivity. Uronic acid binding was too weak to measure, however, with the only exception being D-galacturonic acid with a K_a of 80 M^{-1}.

An important change occurs after the phenanthroline is complexed with zinc. In this case, at a pH of 8.0, the carboxylate functions of the uronic acids can ligate the zinc atom while hydroxyl functions of the saccharide ring can form a boronate ester at the sugar recognition site. Together, these two interactions form a cooperative connection that vastly improves the performance and selectivity of the sensor. The formation of the receptor–saccharide complex yielded a CD active species, which allowed positive determination that the complex was of 1:1 stoichiometry. The generation of a CD-active entity from two CD-silent precursors is a useful feature of this kind of sensor.

Porphyrins, of course, offer excellent platforms for generating CD-active chromophores [16,17]. Furthermore, the sensitivity of CD spectroscopy can allow the determination of precise relative orientations of the electric transition dipoles, which can shed important light on substrate and host conformations. Ogoshi and co-workers [49] have developed their naphthohydroxy porphyrin system (Fig. 15) to behave as just such a sensor.

As previously mentioned [36,37], cooperativity in this system arises from the interaction of the amine nitrogen with the porphyrin-coordinated zinc atom and hydrogen-bonding between the naphthohydroxyl group and the amino acid carbonyl function. In this case, the two point binding immobilises the amino acid above the plane of the porphyrin rendering the whole complex CD active and consequently allowing the detection of hydrogen bonding by CD activity. Immobilisation of the amino acids resulted in a characteristic split Cotton effect (a strong peak and trough in the Soret band) arising from the interaction between the carbonyl group and the porphyrin ring. The intensities of the CD peaks indicated binding strength whilst the sign of the short and long wavelength peaks indicated in which orientation the carbonyl function was lying.

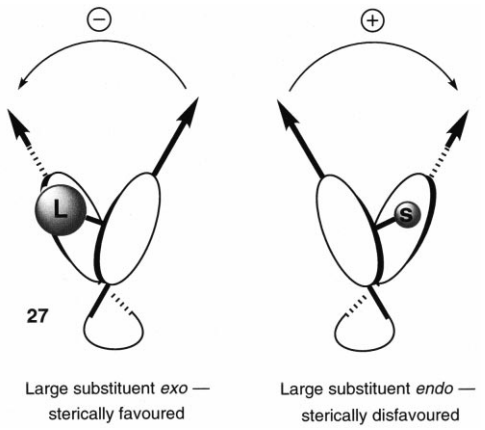

Fig. 23. Detection of the absolute chirality of bidentate ligands through measuring the twist in a porphyrin tweezer.

This same system was later used as a model to study the origin of induced CD in hemeoproteins [50]. Once the mechanism of circular dichromic activity induced in hemeoproteins is known, CD spectroscopy can be used as a highly sensitive probe of the immediate environment of the heme unit. By comparing the behaviour of a number of substrates with varying aromatic and carbonyl structures the study concluded that the main source of CD activity in myoglobin arose from coupling to surrounding aromatic side chains as opposed to carbonyls in the amide backbone. In model studies of human oxy-, deoxy- and methemoglobin, only one of the substrates tested was able to induce a similar magnitude of CD activity as that of the full hemeoprotein, suggesting that the hemeoprotein CD probably arises from the superimposition of many effects. Although the experiments showed that coupling to a carbonyl function makes a greater contribution to CD intensity than coupling to aromatic side-chains, the authors claim that this is because the carbonyl functions are spatially fixed in the model, which is not the case for the more flexible protein backbone, and no CD coupling is observed when the carbonyl functions are allowed to rotate — aromatic groups, however, can make a contribution even when they are free to rotate. Furthermore, the authors believe that the side-chain aromatic groups in the vicinity of the heme unit may be fixed in position by the protein structure, which will increase their contribution to the induced CD effect.

A system that allows absolute detection of chirality has been recently published by Nakanishi et al. [18]. Two zinc porphyrins are linked by a pentanediol chain to form a tweezer assembly with the ability to bind bidentate ligands (Fig. 23). When the ligand contains a chiral centre a twist is induced in the tweezer, which corresponds directly to the absolute chirality of the substrate — this twist can be read in the form of CD exciton coupling.

This system is especially well adapted to chiral diamines but with simple high-yield derivations, it can also be applied to amino acids and amino alcohols. Larger differences in size between the (*S*)- and (L)- groups induce larger CD intensities.

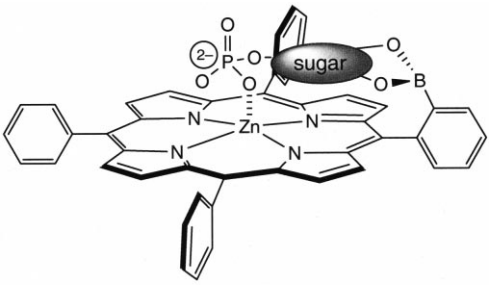

Fig. 24. Cooperative sugar phosphate binding through Zn-phosphate binding and boronic ester formation.

Once again, using boronic acid for saccharide recognition, phosphate derivatised saccharides were able to coordinate to the central zinc atom of a metallated porphyrin as shown in Fig. 24 [51]. Boronic acid was used to provide the complementary cooperative binding site that promotes discrimination between phosphate substitution patterns.

^{31}P-NMR indicated that glucose-6-phosphate (G-6-P) is bound more strongly to the porphyrin than is glucose-1-phosphate (G-1-P) (Fig. 25) and CD spectroscopy confirmed two point binding of the G-6-P complex. The binding constants in MeOH were found to be 1.5×10^3 M^{-1} for the G-6-P case and 0.25×10^3 M^{-1} for G-1-P. D-Glucose was CD silent but no binding experiments were performed.

Having established selectivity for glucose phosphates, the related behaviour of L-dihydroxyphenylalanine (L-DOPA) was also investigated. The catechol moiety of L-DOPA is known to form one of the strongest associations with boronic acids while the amine function has the ability to ligate to the zinc atom, which should lead to cooperative binding.

Guests containing the catechol function showed association constants larger than 1000 M^{-1} whilst those without the catechol moiety showed either low binding or none at all. In methanol, DOPA and dopamine, containing zinc ligating ability, had binding constants of 57- and seven-fold larger than catechol, respectively, whilst

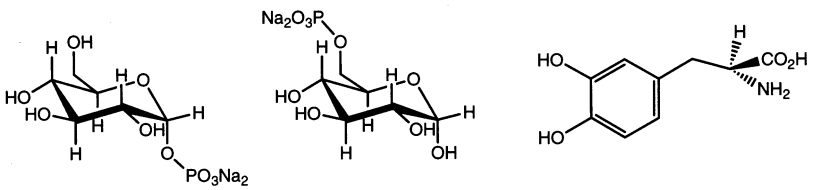

29 **30** **31**

Fig. 25. Sugar phosphate derivatives and L-DOPA used to investigate the binding affinity of the boronic acid appended porphyrin (Fig. 24).

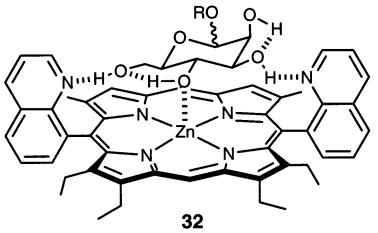

32

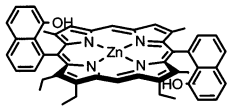

33

Fig. 26. The *cis*-quinyl porphyrin with bound mannose. The *trans*-hydroxy version is also illustrated.

CD spectroscopy once again confirmed the two-point fixation of these guests. Binding constants measured in MeOH–water, however, were very similar, suggesting that the cooperative boronic acid interaction was of chief importance in attaining selectivity in non-polar media, although CD spectroscopy indicated that the Zn–N interaction plays an important part in immobilising the substrate.

The naphthylhydroxy porphyrin [37] (Fig. 15) and a related naphthoquinyl porphyrin (Fig. 26) of Ogoshi and co-workers [52] was also found to complex diols and carbohydrates. The binding constants were consistently higher for the *cis*-quinyl type and decreased thereafter in the order *trans*-quinyl- > *cis*-hydroxy- > *trans*-hydroxyporphyrin. Split Cotton effects, indicative of the substrate being held rigidly in the porphyrin plane, were observable for certain combinations of substrate and porphyrin but CD intensity did not correspond to binding strength, suggesting that immobilisation was similarly independent of binding strength.

Worthy of particular note is the fact that the absolute orientation of carbohydrates rigidly bound on the porphyrin plane could be inferred from their induced CD patterns when coupled with computer modelling of the substrate electronic orbitals.

Alternative methods of orienting the recognition sites have also been explored [53]. In this case, rather than fix a pair of boronic acids rigidly to the porphyrin skeleton, one of the sugar recognition sites is appended to a free pyridine ring, which itself coordinates to the central zinc atom (Fig. 27). The binding constant for the pyridine moiety **34b** with the porphyrin **34a** was found to be 4.7×10^4 M^{-1} in CH_2Cl_2, typical of most interactions between pyridine and Zn-metallated porphyrins.

Because of the possibility of generating many species within a homogeneous solution of porphyrin, pyridine and saccharide, the extraction of solid saccharide into dichloromethane solution was examined. Mixtures of **34b** and free base **34a** were not able to extract any saccharide at all, nor were mixtures of **34b** and tetraphenylporphyrin. A mixture of **34b** and zinc-metallated **34a** was able to extract

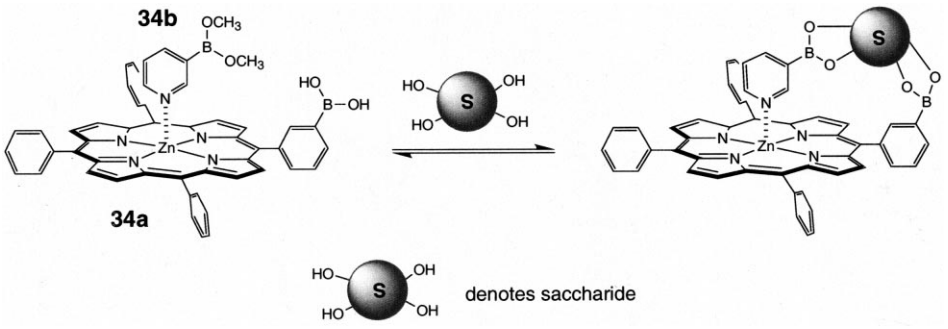

Fig. 27. Metal ion coordination is used to assemble binding sites in a convergent manner before co-operating to selectively bind carbohydrates.

saccharides and gave CD spectra related to the saccharide absolute configuration. Although the most lipophilic saccharides were extracted preferentially, there was still a large difference between the proportion of fucose extracted (97 and 85% for D- and L-enantiomers, respectively) and xylose (D-enantiomer, 2%), even though both are lipophilic saccharides. This difference was attributed to the favourable pattern of *cis*-diols in fucose, which is absent for xylose. Extractions using high concentrations of building blocks were also much less efficient as a result of competing binding connectivities — the most striking difference being a decrease from 97% extraction for D-fucose at low concentration (**34a**, 4×10^{-6} M; **34b**, 2.1×10^{-3} M) to only 30% at higher concentration (**34a** = **34b** = 2.1×10^{-3} M).

Another method that involves preassociation to form the complete receptor was based on dimer formation between anionic **35** and cationic **36** porphyrins [54] (Fig. 28). Continual concentration variation plots indicated the formation of a 1:1 porphyrin dimer. CD activity was not observed in the absence of saccharides but was observed in the presence of glucose and xylose and since a single saccharide cannot span two boronic acids of the same porphyrin ring, the CD activity was ascribed to linkage between the porphyrins within a dimer. CD activity was not observed for other saccharides but this behaviour could not be satisfactorily explained.

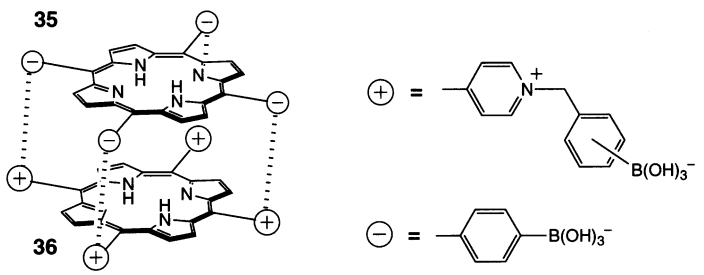

Fig. 28. Boronic acid appended porphyrin dimer formed through electrostatic attraction.

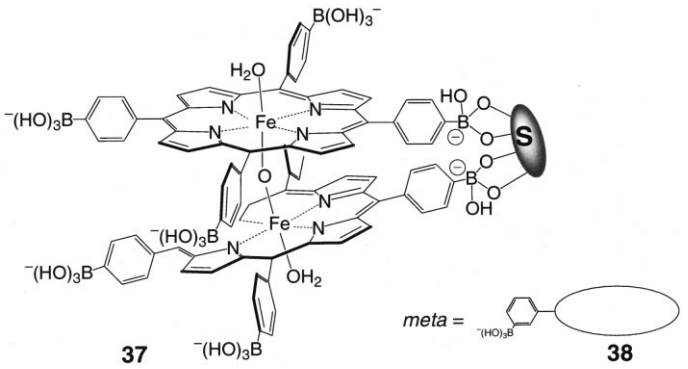

Fig. 29. A μ-oxo porphyrin 'double-decker' complex capable of binding carbohydrates through peripheral boronic acid groups.

The porphyrin dimer motif was refined later to make use of a stronger covalent linkage to join the porphyrin rings [55]. Using an iron metallated μ-oxo porphyrin dimer, peripheral boronic acid groups on adjoining porphyrins can come together when linked by a saccharide (Fig. 29). This interaction, in turn, immobilises the saccharide inducing CD activity in the overall complex. Two isomers were synthesised, **38** which has boronic acids in the *meta*- positions on the phenyl rings and **37** with the acids in the *para*-positions. **38** was not found to make any CD active complexes while **37** could form CD active complexes only with glucose and galactose. The inability of **38** to form CD active complexes was attributed to the ability of the *meso*-phenyl rings to rotate slightly even when bound, allowing the porphyrins some freedom of movement — this slight rotation presumably cannot occur in **37**. Weak CD spectra were obtained for disaccharides with both isomers, though their extra flexibility, gained from the central glycoside linkage, prevented proper imagery of the nature of the bound complex.

Even though strong binding constants were measured for the complex of **37** with D-glucose (1.51×10^5 M^{-1}) and galactose (2.43×10^4 M^{-1}) in H_2O, pH 10.5, the complexes were established by continual variation plots to be of only 1:1 stoichiometry, indicating an allosteric effect, which will be discussed in more detail below. Competition experiments revealed the selective nature of this sensor with only glucose and galactose being able to compete for binding sites. CD studies suggested that the 4-OH group of these two species is responsible for controlling the orientation of the bound saccharide, though ^{1}H-NMR spectroscopy could not be used to establish absolute configurations as a result of line broadening caused by the Fe(III) ions.

Another method of utilising CD activity for sensing applications is to make the sensor itself chiral and monitor the changes brought about by complexation with achiral guests. A convenient route to chiral chromogenic receptors is to link two porphyrins with a chiral bridge. An example of this approach, produced by Crossley et al., appears in Fig. 30 [56].

The chiral linker imparts a twist to the porphyrin dimer that influences chiral recognition while the cleft and pair of zinc atoms constitute a three-point binding interaction when complexing diamines such as histidine esters. The receptor itself shows symmetrical split Cotton effects in its CD spectrum and the absolute stereochemistry of each optical isomer can therefore be established. ^{1}H-NMR spectroscopy indicated slow exchange of ligands and also that L-histidine had a clear preference for binding to the (+) optical isomer with a selectivity of 86% over the (−) isomer. Furthermore, the bound histidine esters exist in only two stable conformers demonstrating that the host is capable of imparting conformational stability. L-Lysine benzyl ester shows a much smaller selectivity arising from a more flexible backbone though it has weaker binding than 1,5-diaminopentane because of steric repulsion from the benzyl ester group.

A similar design incorporating a binaphthyl chiral linker has also been reported [57]. This complex (Fig. 31) shows a Cotton effect, which increases with strength when binding to diamines of chain lengths between six and 12 methylene groups. Smaller chains and the mono amine *n*-octylamine show weaker Cotton effects. In this case, CD spectroscopy can be used to sense chain length as well as binding.

Another related system using the same principles was simultaneously reported by Ema et al. [58] this time using a chiral cyclophane as spacer (Fig. 32). This sensor demonstrated stronger binding for the diamines in CH_2Cl_3 ($> 10^7$ M^{-1} compared with 5.5×10^5 to 1×10^6 M^{-1} for the binaphthyl linked system) but only showed split Cotton effects for chain lengths of six and seven methylene groups, making this system either more restricted or more selective, depending upon the application.

An alternative method for making a chiral porphyrin is to make asymmetric substitutions around the periphery. This approach has been investigated by the use of nitrophenyl bridging groups (Fig. 33) [59,60]. Nitrophenyl units connected at the 1,4- or 1,3- positions generate *meso* and enantiomeric isomers that differ slightly in cleft shape. The nitrofunction has a different effect on each of its neighbouring

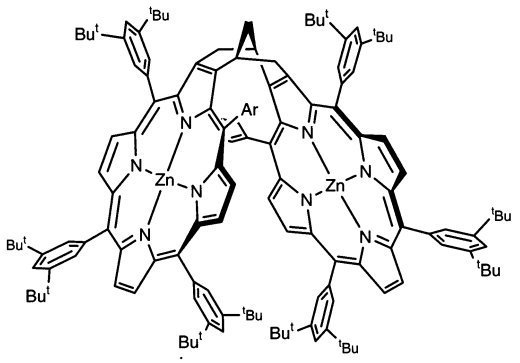

39

Fig. 30. A porphyrin dimer linked by a Tröger's base analogue. This dimer is twisted making the assembly chiral.

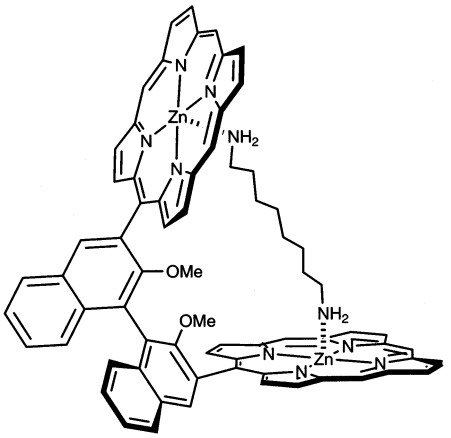

40

Fig. 31. A dimer pair that uses a binaphthyl linker to generate a chiral twist. Using this sensor, CD spectroscopy can be used to estimate the chain length of diaminohydrocarbon chains.

amide groups to which an amino acid can bind through hydrogen bonding interactions between the amino acid ester carbonyl and the amide N–H proton. With L-amino acids in $CHCl_3$, the 1,4-connected isomer showed the weakest binding ($\sim 1 \times 10^3$ M^{-1}) while for the 1,3-connected case, the (+) enantiomer showed weaker binding (1.7×10^3 to 7×10^3 M^{-1}), the *meso* isomer intermediate (2.2×10^3 to 14×10^3 M^{-1}) and the (−) isomer showed the strongest binding

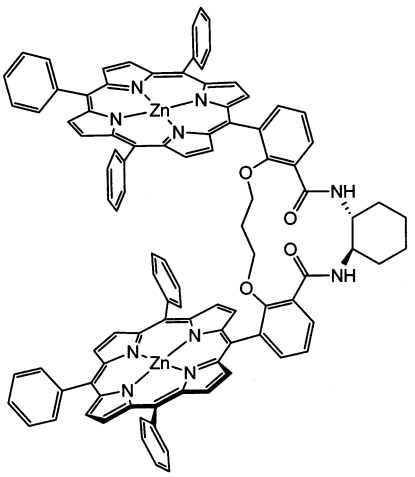

41

Fig. 32. A porphyrin dimer that uses a chiral cyclophane to impart a twist.

(11×10^3 to 22×10^3 M^{-1}). Binding was monitored by red shifts in the Soret band upon complexation. Steric repulsions from porphyrin side-chain substituents were also important in determining binding strength.

3. Developing sensors into selective catalysts

Of course, reactivity and catalysis are actions fundamental to chemistry and so it is not surprising that many systems originally designed as selective sensors have been transformed into chemically active species [61–64]. An example of this concept can be seen in the doubly cyclodextrin-capped porphyrin discussed above [32] (Fig. 10). This molecule can operate in two modes, as a sensor that signals a binding event through UV absorption and as an oxidative catalyst that uses the same binding event to trap a substrate near an activated iron centre. In the catalysis study, a number of hydrophobic alkenes were treated with a mixture of **14** and iodosobenzene as the preliminary oxidising agent [65] to generate the corresponding epoxides. A simple tetrasulphonic acid-derivatised porphyrin was used as a non-binding water soluble model compound. Although the studies showed fairly low yields of oxidation using the capped porphyrin (14%) the model porphyrin showed almost no oxidation for cyclohexene (cf. 55% for **14**). Both systems generated the same yield of epoxide for 2,3-dimethylbut-2-ene but this result was not discussed. The difference in epoxidation yields in the case of cyclohexene was attributed to the solubilising effect of the cyclodextrin cavities since the reaction is otherwise heterogeneous because of the poor solubility of the alkenes in water. The reactive porphyrin oxene intermediate of the control compound was thought to decompose before it could react at the cyclohexene–water interface while the cyclodextrin-complexed cyclohexene could be oxidised in a manner analogous to a homogenous reaction. An alternative explanation, where the oxene intermediate of the capped

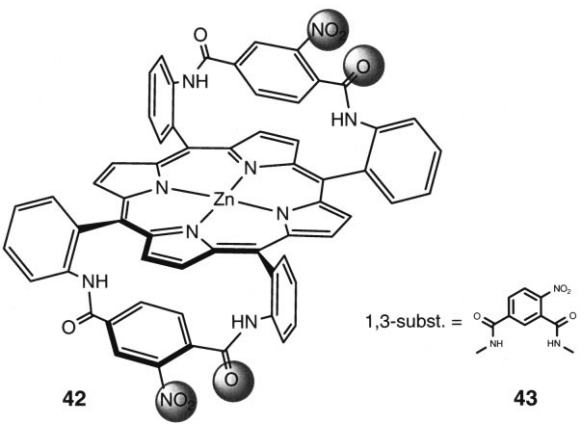

42 43

Fig. 33. A chiral, strapped porphyrin. Selectivity is achieved chiefly through the inductive influence of the NO_2 group on its local amide carbonyl function.

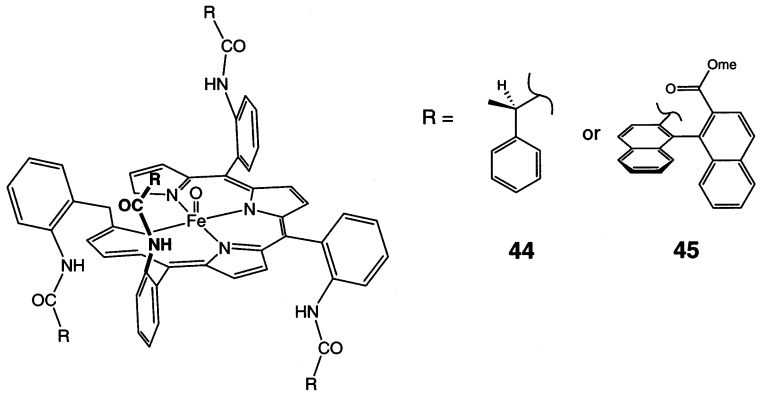

Fig. 34. Two catalytically active picket fence porphyrins containing a chiral cavity. Only the *trans*-α^2 atropisomer is shown.

porphyrin is protected by the hydrophobic caps, thus allowing its transport to the organic–aqueous interface, was briefly mentioned. Thus a sensor assembly can be used directly as a chemical action platform, in this case, a catalyst for oxidation.

Porphyrins with chiral buttresses have been studied extensively as selective catalysts. Such a system was originally reported by Groves and Myers [66] (Fig. 34) using a pivalamido picket fence porphyrin to effect achiral epoxidations. The alternate α-β-α-β-porphyrin produced oxidation products in reasonable yields of around 60% but with low enantiomeric excesses (e.e.s) of 10%. The other atropisomers gave only racemic products, presumably from a lack of steric effects on one of the faces.

The same study also considered the use of a binaphthyl buttressed porphyrin. The yields for this porphyrin were also reasonable, being in the range of 58% but higher e.e.s were observed, ranging from 7% with the e.e.s being strongly dependent upon the nature of the alkene. However, The catalyst was observed to deactivate over time, which, although indicating that e.e.s may be higher for early reaction times, seriously limits this porphyrin's ability to act as a catalyst.

A porphyrin with binaphthalene chiral walls has been briefly considered [67] for the enantioselective epoxidation of small alkenes but was found to result in only low enantiomeric excesses (Fig. 35). In this case, it was considered that the chiral walls do not co-operate to a sufficient degree to greatly influence small molecule oxidation.

More impressive enantioselectivities were obtained for a related binaphthyl 'coronet' system (Fig. 36) where the binaphthyl moieties joined adjacent phenyl groups [68]. Yields were reported as 26% with the (*R*)-epoxides being formed in e.e.s between 0 and 80% with the best yields being for alkenes bearing electron deficient groups.

A similar coronet system using threitol substituents has been reported by Che et al. [69] who reported high e.e.s of up to 76% with concomitant, high, isolated yields

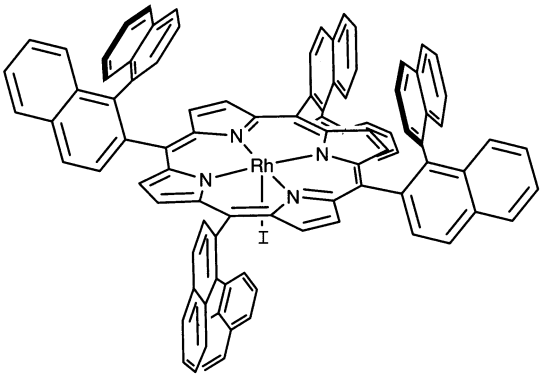

46

Fig. 35. A chiral porphyrin using binaphthyl moieties to form a chiral cavity.

of around 70%. They also reported an unusual 'head-on' approach of the substrate to the reactive centre as indicated by the facial selection of *trans*-alkene epoxidation.

An oxidising system using porphyrins with chiral appendages has also been used [70] to achieve a modest enantiomeric excess in the dioxygen oxidation of racemic *N*-acetyl-tryptophan to its ring-opened derivative. Selectivities were found to depend on the nature of the chiral arms and the atropisomer but not on the oxidation state of the central manganese ion. Yields, however were dependent on the manganese oxidation state with the manganese(II) ion generating the highest yield of 10.4%. The highest e.e. determined was 23.3% in favour of the D-product performed by the α^4-configured porphyrin with a yield of 6.1%.

Although hydrogen peroxide is cheap and yields only water as a side-product, it is usually too strong for most porphyrin catalysed applications. Using glycosylated side walls and chlorosubstituents on the pendant phenyl rings, a chiral porphyrin

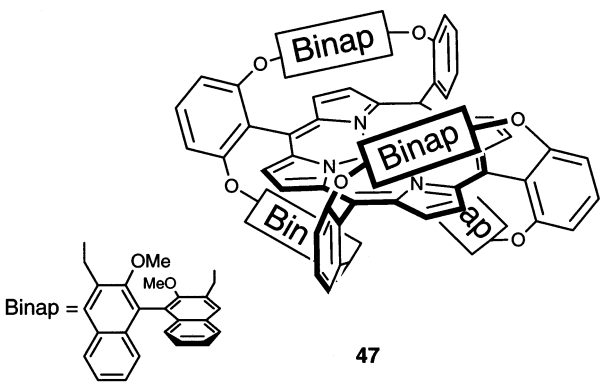

47

Fig. 36. A BINAP coronet porphyrin that encloses a catalytic photoactive site within a chiral cavity.

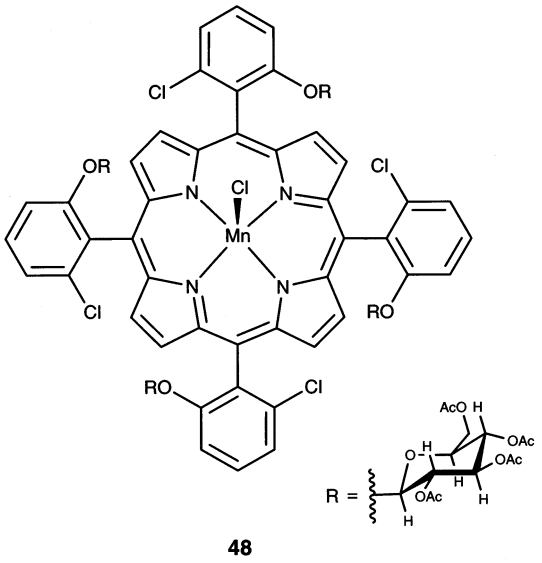

48

Fig. 37. A porphyrin catalyst, stable to hydrogen peroxide, that makes use of glycosylated side chains to form a chiral cavity.

has been constructed that can function even in the presence of H_2O_2, allowing relatively expensive oxidising agents to be dispensed with [71] (Fig. 37). Better yields were obtained with iodosobenzene, however, and, in this case, **48** was able to catalyse the oxidation of 4-chlorostyrene in modest yields (25%) with modest e.e. ($\sim$20%).

A more efficient design made use of a strapped porphyrin to present diastereotopic faces to potential substrates, thus promoting asymmetric epoxidation [72]. Imidazole is required to block the unstrapped face of the porphyrin to prevent facile oxidation without stereocontrol (Fig. 38) and typical yields were of the order of 43% with a 49% e.e. CD spectroscopy was used to determine that the (+) form of the porphyrin consistently generated (*R*)-epoxides in excess and (−) forms consistently generated (*S*)-epoxides in excess. When epoxidation without imidazole or with a weaker coordinating base was performed the substrates could react in any orientation at the free face and so e.e.s were significantly reduced. The nature of the straps were also important, with the *p*-substituted xylyl strap providing the greatest enantioselectivities followed by the *m*-substituted strap and the flexible aliphatic strap providing the least selectivity of all. Competition experiments demonstrated that the least sterically hindered epoxides were preferentially oxidised, which was further evidence for the inclusion of the alkenes within the strap cavity.

Reasonably good e.e.s were also obtainable using a cyclodextrin appended porphyrin (Fig. 39) [73]. The chiral cavity of the cyclodextrin is able to discriminate in its complexation of α-pinenes and this was expected to lead to an enantioselectivity in oxidation of this compound. Oxidation was achieved simply by irradiating the

solution with visible light in the presence of air. Different oxidation product distributions and e.e.s were obtained in different solvents and between the Mn and Fe metallated porphyrins but the (*S*)-products were always formed in excess. The greatest e.e.s were obtained in polar solvents, presumably a consequence of greater substrate binding within the hydrophobic cavity leading to enhanced selectivity. The addition of a coordinating base such as 2-methylpyridine also enhanced the selectivities by coordinating to the non-selective free face of the porphyrin but forced complexation of the remaining substrates led to lower turnover numbers.

The most significant development to date, however, has been reported by Collman and co-workers [74]. Returning to the binaphthyl cross-linked theme of Maruyama et al. [68] (Fig. 36), they attached only two binaphthyl bridges in an α-α-β-β arrangement. This small but important change allowed greater substrate access to the porphyrin active centre whilst still maintaining a bulky steric environment; resulting in not only higher e.e.s (82% for styrene derivatives) but also greater catalytic turnover ($\sim$ 5500 turnovers at 40 min^{-1}) and stability. In the initial stages of the reaction, the e.e.s were actually observed to increase and after further investigation the authors attributed this behaviour to the formation of a more efficient self-oxidised form of the catalyst that is actually responsible for the main behaviour of this system.

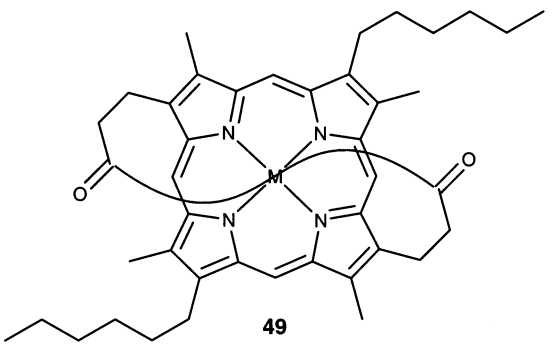

49

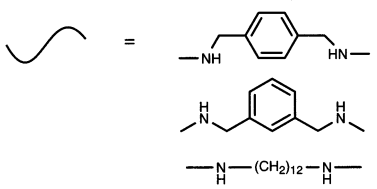

Fig. 38. Use of an achiral strap to render a catalytic porphyrin with enantiomeric faces. A competitive base must be used to block the free face of this porphyrin so that substituents are forced to interact with the strapped side of the catalyst.

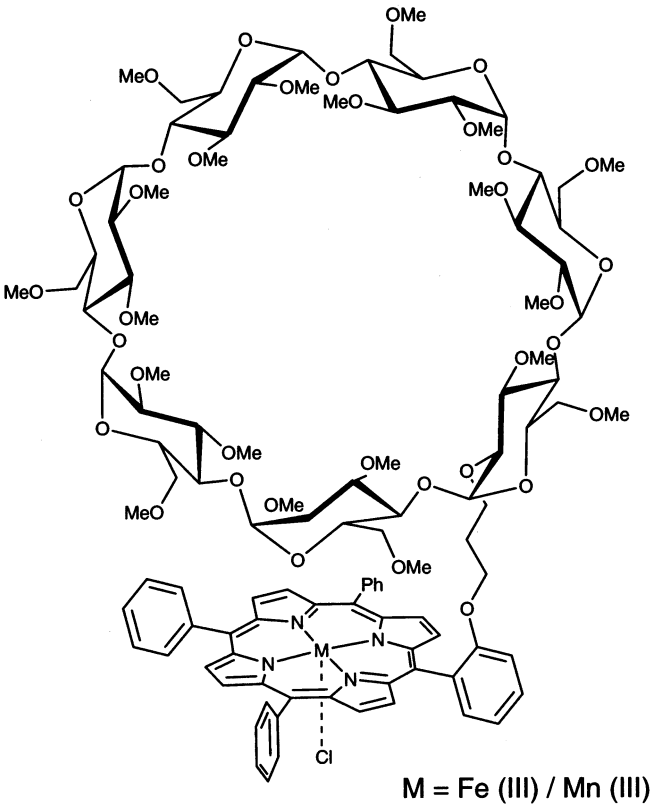

50

Fig. 39. A cyclodextrin appended porphyrin capable of selectively oxidising α-pinenes.

4. Developing sensors into actuators

The same design considerations used to construct selective sensors can be applied to the construction of molecular devices used to perform a mechanical function such as selective transport [75–77]. A good example of the crossover in these concepts can be found in the sugar–tweezer sensor discussed above [55] (Fig. 29). The tweezer was observed to form only a 1:1 complex with saccharides despite having four potential binding sites, which has been attributed to a form of negative allosterism. Allosterism is a form of chemical feedback, found in many biological processes [78–80], and artificial systems [81,82] where initial binding of a substrate has a positive or negative effect on subsequent binding events.

In the case of the sugar tweezer, complexation of the first saccharide pulls two boronic acids together thus 'tilting' the two porphyrins in the dimer. This tilting effect pulls the remaining binding sites apart, which prevents further saccharide binding. This is an example of a sensor that can also function simultaneously as a negative allosteric device.

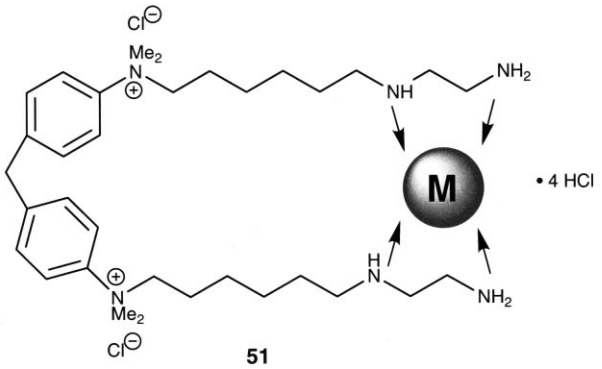

Fig. 40. A heteroallosteric system. A metal ion template is required to assemble the flexible chains into a cavity which can then complex fluorophores. Paramagnetic and diamagnetic ions can be differentiated by their influence on the fluorescence.

Allosteric interactions can be used directly to influence sensor behaviour. A sensor containing a flexible chain as illustrated in Fig. 40 can be assembled to form a cavity by the addition of a coordinating metal, in this case either zinc or copper ions [83]. Fluorophores can bind within the hydrophobic cavity where they are shielded from the quenching effect of water [84]; this results in an increase in fluorescence but only as a result of allosteric binding between Zn and the fluorophore. This system has the potential to act as a sensor for diamagnetic transition metal ions as a result of their high affinity for this ligand and the sensitivity of fluorescence spectroscopy. Paramagnetic ions, however, cause fluorescence quenching and can therefore be easily differentiated.

Fig. 41 illustrates a related water-soluble sensor that relies on the allosteric binding of a calcium cation and a fluorophore [85]. When two aminodicarboxylate

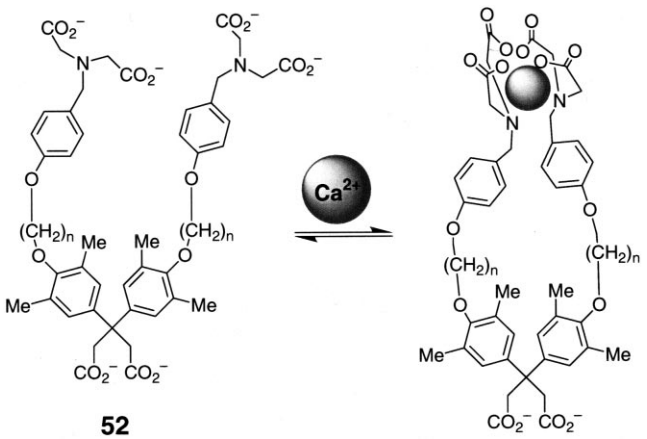

Fig. 41. An allosteric system that uses a calcium ion to form a cavity suitable for binding fluorophores.

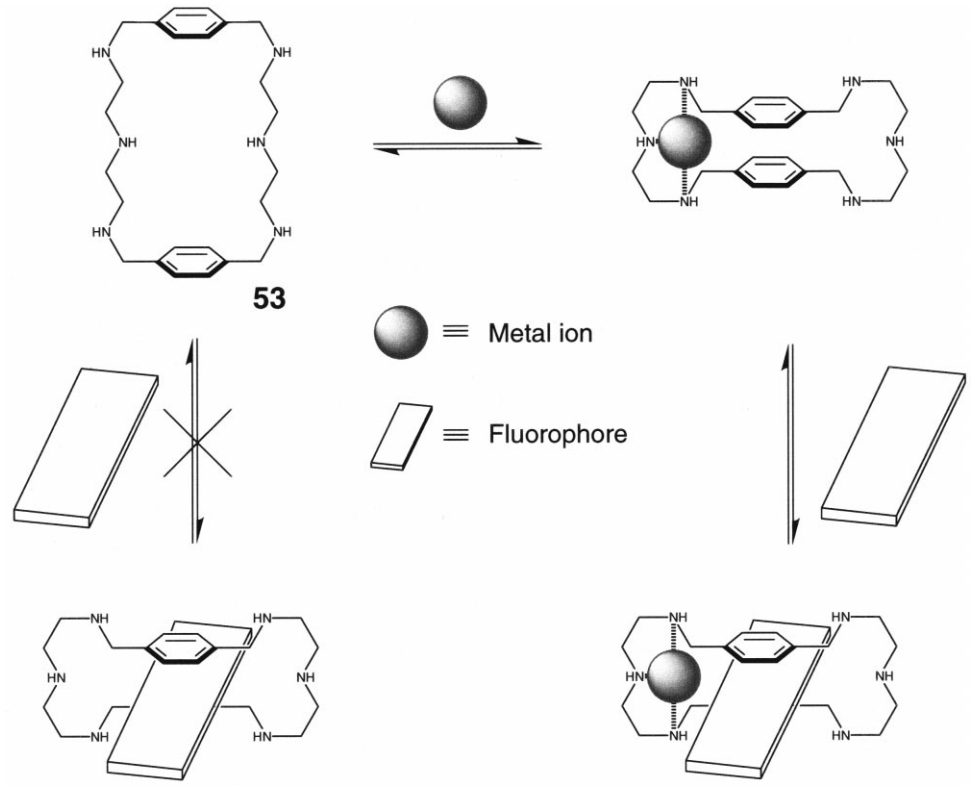

Fig. 42. An allosteric system dependent upon metal ion binding to organise a cavity for inclusion of a fluorophore.

moieties intramolecularly bind to a calcium cation they create a hydrophobic cavity that can complex fluorophores such as 6-(toluidino)-2-naphthalenesulphonic acid (TNS). The fluorescence of TNS in aqueous solutions is low but it can be restored by enclosure within a hydrophobic cavity. The 'proto-cyclophane', therefore, requires TNS to be fluorescent, while the TNS cannot bind without calcium to form the binding pocket. This constitutes a positive, heterogeneous allosteric effect.

The theme was continued by the introduction of a system that also relies on Zn ion binding to preorganise a flexible, preformed macrocycle (Fig. 42) which increases fluorescence of a fluorophore guest by complexation [86]. Although this host has two metal binding sites, only one ion coordinates at a time. The singular binding is credited to the deformation of the second site upon binding of the lipophilic fluorophore.

A design that simply couples a dibenzocrown ether with a pair of boronic acids [87] is illustrated in Fig. 43. The free macrocycle preorganised the boronic acids for better binding to D-glucose and D-talose, which could be monitored by CD spectroscopy. This preorganisation could be significantly disrupted by the addition

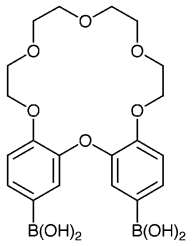

54

Fig. 43. A simple negative allosteric system. Complexation of a metal ion within the macrocycle prevents the boronic acids from forming a suitable geometry for binding saccharides.

of suitable cations, such as potassium and calcium, resulting in negative allosterism for the anticooperative binding of these cations and D-allose. Calcium had the largest allosteric effect which was considered to be the result of extra stabilisation of the metal complex arising from the interaction of the double positive charge with the two negative charges on the boronic acids (the experiment was preformed at pH 11.6 where boronic acid moieties exist as $B(OH)_3^-$).

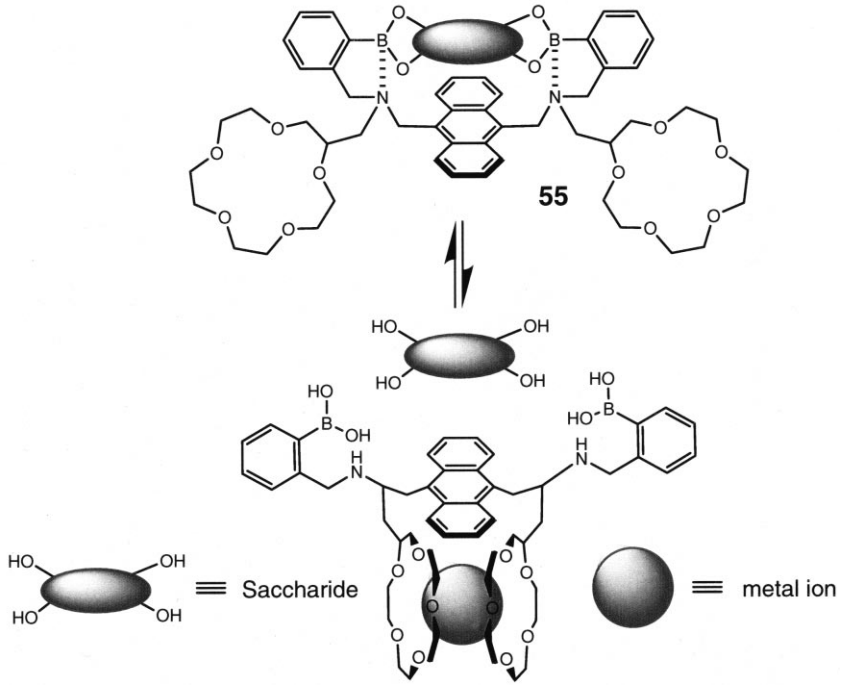

Fig. 44. A negative allosteric system that is unable to bind saccharides in the presence of certain metal ions as a result of disruption of the necessary binding geometry.

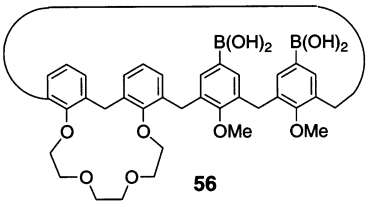

Fig. 45. A negative heterogeneous allosteric system based on communication between the lower and upper rim of a calixarene.

The design was then developed to perform heterotopic negative allosterism where the receptor itself is a fluorophore (Fig. 44) and can consequently be used to act as a sensor for saccharides that functions only in the absence of certain alkali and alkaline earth cations [88]. Although the central anthracene moiety has a capacity for fluorescence, the neighbouring methylamino groups quench this fluorescence through a PET interaction similar to that described above for the phenanthroline–boronic acid linked fluorophore [48] (Fig. 22). When a saccharide binds to the sensor, the nitrogen lone pairs coordinate to the boronic acid and a fluorescence increase is observed. When hard cations that can form a sandwich complex with the pendant crown ethers are added, however, the boronic acid receptors are forced apart, the complex dissociates and fluorescence is quenched. Lithium and caesium, ions that are too small and too large, respectively, to form sandwich complexes, show no fluorescence quenching behaviour. Therefore, the fluorescence emission can be controlled by the presence or absence of particular cation co-factors.

Another example of this form of allosterism was designed around a central calix[4]arene core (Fig. 45) [89]. Boronic acid receptors are attached to the upper rim of the calixarene and a crown ether to the bottom. Calixarenes with receptors grafted at the lower rim [90] are known to change conformation upon metal complexation [91,92] and so the boronic acid receptors were expected to move apart upon metal complexation in a similar manner to the system in Fig. 44 [88]. CD activity was observed when **56** was added to solutions of D-glucose, which increased until it reached a plateau at around 1.8 equivalents of saccharide. The intensity could be reduced by the addition of small cations such as Na^+, Mg^{2+} and Ca^{2+} indicating that complexation at the lower rim disrupted the favourable binding geometry at the upper rim. Addition of larger cations such as K^+ and Cs^+ actually increased the CD intensity above its original value. This behaviour was attributed to the formation of a 1,2-alternate calixarene conformation which sandwiches the ions between the crown and two phenyl rings and is actually more favourable for sugar binding. The overall system could therefore be switched between positive cooperativity for sugar binding and negative cooperativity by the choice of suitable metal ions.

Chiral transcription is another task that can be performed by interacting molecules [93]. The concepts utilised to generate chirally selective sensors can also be used to transfer a chiral configuration to achiral building blocks which are then potentially able to signal this information through their spectroscopic properties.

Sugars are naturally abundant sources of chiral information and receptors carrying recognition functions capable of binding in an ordered manner can potentially read and store this information. An example of this kind of device appears in Fig. 46 [94].

The bipyridine ligand was observed to form CD active species with certain D-saccharides as a result of a twist induced in the plane of the bipyridyl rings, dependent of the saccharide's ability to bond to both boronic acid moieties simultaneously. Bipyridyl ligands form inherently chiral complexes with metal centers in either a Δ or a Λ form. When mixed with Fe(II) ions in solution, the bipyridine ligand formed a species with strong CD activity but the sign of the CD bands could be reversed easily by the addition of the enantiomeric saccharides, demonstrating a labile complex with little use for transcription. An alternative methodology that involved chiral transcription to a labile Co(II) complex followed by oxidation to the inert Co(III) complex was therefore pursued. The transcription and fixing ability was tested by (i) mixing the ligands, metal and saccharide followed by oxidation and (ii) mixing the saccharides with a pre-oxidised Co(III) complex. Although both mixtures showed CD activity after oxidation, addition of *cis*-cyclopentane-1,2-diol, a competitive inhibitor of the saccharide–boronic acid interaction, reduced the CD activity of the control system (ii) to zero but left residual CD activity in the case of the test system (I). The highest optical yields were obtained by using glucose for transcription and at lower temperatures. At −25°C an e.e. of 79% Δ-complex was observed. The mechanism of the transcription is not yet clear but is thought to rely on interligand bridging by the saccharide to favour the Δ-enantiomer.

This idea naturally extends to helicity control [95]. Phenanthroline ligands with boronic acid functions positioned at the termini could be expected to form helicates with their chiral twists determined by sugar recognition — Fig. 47 illustrates just such a ligand. Upon mixing this ligand with Cu(I) ions and D-glucose, a CD active

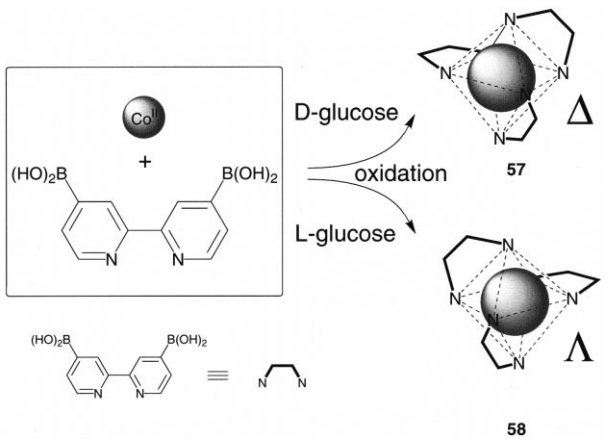

Fig. 46. Chiral transcription from a sugar to a stable cobalt complex.

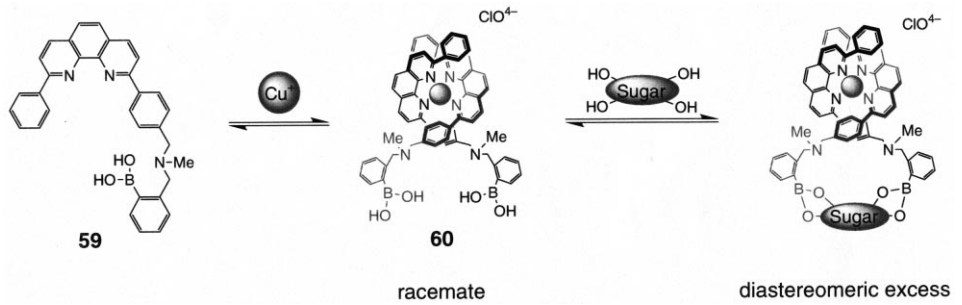

Fig. 47. A saccharide can be used to transfer chiral information in the form of a diastereomeric excess in a boronic acid appended helicate. A copper ion templates initial formation of a racemic mixture of the helicate which is then converted to a diastereomeric excess through the reversible binding of a saccharide (only the P-isomer shown).

species became apparent, signifying the appearance of a chiral excess. The positive sign of the first Cotton effect indicated that the helicate was present in the clockwise P form. Studies with other saccharides suggested that the chirality of the 3-OH group determined the twist of the helix such that the D-enantiomers of glucose, mannose, fucose, galactose and xylose induced formation of the P-helix whilst D-arabinose and D-allose induce H-helicity.

5. Conclusions

The systems discussed in this account provide a sample of systems that use the principles of multiple, concerted, intermolecular interactions to enhance selectivity and binding for a range of applications. The incorporation of metal ions provide additional tools for use as coordinating Lewis acids or for providing a source of hard, positive electrostatic charge to induce conformational changes. When combined within a single receptor, these features give the chemist great scope in the rational design of devices with applications that translate smoothly from selective sensors to selective catalysts and actuators. The conceptual designs presented in these pages will undoubtedly form the foundations for future devices capable of remarkable advances in molecular technology.

Appendix A. Abbreviations

CD	circular dichromism
e.e.	enantiomeric excess
L-DOPA	L-dihydroxyphenylalanine
NMR	nuclear magnetic resonance
PET	photoelectron transfer
TNS	6-(toluidino)-2-naphthalenesulphonic acid
UV–vis	ultraviolet–visible

References

[1] J.L. Meinershagen, T. Bein, J. Am. Chem. Soc. 121 (1999) 448.
[2] A.W. Czarnik, Acc. Chem. Res. 27 (1994) 302.
[3] For some examples, see: (a) S. Nishizawa, H. Kaneda, T, Uchida, N. Teramae, J. Chem. Soc. Perkin Trans. 2 (1998) 2325. (b) K. Niikura, A. Metzger, E.V. Anslyn, J. Am. Chem. Soc. 120 (1998) 8533. (c) L. Fabbrizzi, I. Faravelli, G. Francese, M. Licchelli, A. Perotti, A. Taglietti, Chem. Commun. (1998) 971. (d) P.D. Beer, Chem. Commun. (1996) 689. (e) R.V. Slone, D.I. Yoon, R.M. Calhoun, J.T. Hupp, J. Am. Chem. Soc. 117 (1995) 11813.
[4] For an excellent review of metal based receptors, in general, see: J.W. Canary, B.C. Gibb, Prog. Inorg. Chem. 45 (1997) 1.
[5] P.D. Beer, Acc. Chem. Res. 31 (1998) 71.
[6] V. W-W Yam, K. K-W. Lo, K-K. Cheung, Inorg. Chem. 34 (1995) 4013.
[7] S.C. Rawle, P. Moore, N.W. Alcock, J. Chem. Soc. Chem. Commun. (1992) 684.
[8] J. Bourson, J. Pouget, B. Valuer, J. Phys. Chem. 97 (1993) 4552.
[9] I. Aoki, T. Sakaki, S. Shinkai, J. Chem. Soc. Chem. Commun. (1992) 730.
[10] S. Zhao, J.H.T. Luong, J. Chem. Soc. Chem. Commun. (1995) 663.
[11] A. Hamilton, J-M Lehn, J.L. Sessler, J. Am. Chem. Soc. 108 (1986) 5158.
[12] M. Shionoya, E. Kimura, M. Shiro, J. Am. Chem. Soc. 115 (1993) 6730.
[13] A.P. de Silva, K.R.A.S. Sandanayake, Angew. Chem. Int. Ed. Engl. 29 (1990) 1173.
[14] J.L. Sessler, B. Wang, A. Harriman, J. Am. Chem. Soc. 117 (1995) 704.
[15] N. Harada, K. Nakanishi, Circular Dichromic Spectroscopy — Exciton Coupling in Organic Stereochemistry, University Science Books, Mill Valley, MA, 1983.
[16] S. Matile, N. Berova, K. Nakanishi, J. Am. Chem. Soc. 117 (1995) 7021.
[17] T. Ema, S. Nemugaki, S. Tsuboi, M. Utaka, Tetrahedron Lett. 36 (1995) 5905.
[18] X. Huang, B.H. Rickman, B. Borhan, N. Berova, K. Nakanishi, J. Am. Chem. Soc. 120 (1998) 6185.
[19] H. Ogoshi, T. Mizutani, Acc. Chem. Res. 31 (1998) 81.
[20] J.S. Lindsey, R.W. Wagner, J. Org. Chem. 54 (1989) 828.
[21] T. Nagasaki, H. Fujishima, M. Takeuchi, S. Shinkai, J. Chem. Soc. Perkin Trans. 1 (1995) 1883.
[22] J.L. Sessler, E.A. Brucker, Tetrahedron Lett. 36 (1995) 1175.
[23] H. Imai, E. Kyuno, Inorg. Chem. 29 (1990) 2416.
[24] J.P. Collman, R.R. Gagne, C.A. Reed, T.R. Halbert, G. Lang, W.T. Robinson, J. Am. Chem. Soc. 97 (1975) 1427.
[25] J. Odo, H. Imai, E. Kyuno, K. Nakamoto, J. Am. Chem. Soc. 110 (1988) 742.
[26] H. Imai, S. Nakagawa, E. Kyuno, J. Am. Chem. Soc. 114 (1992) 6719.
[27] H. Imai, Y. Uemori, J. Chem. Soc. Perkin. Trans. 2 (1994) 1793.
[28] A. Blaskó, B. Garcia, T.C. Bruice, J. Org. Chem. 58 (1993) 5738.
[29] J.P. Collman, X. Zhang, P.C. Herrman, E.S. Uffelman, B. Boitrel, A. Straumanis, J.I. Brauman, J. Am. Chem. Soc. 116 (1994) 2681.
[30] R. Nakamura, A. Ikeda, L.D. Sarson, S. Shinkai, Supramol. Chem. 9 (1998) 25.
[31] D.R. Benson, R. Valentekovich, C.B. Knobler, F. Diederich, Tetrahedron 47 (1991) 2401.
[32] Y. Kuroda, T. Hiroshige, T. Sera, Y. Shiroiwa, H. Tanaka, H. Ogoshi, J. Am. Chem. Soc. 111 (1989) 1912.
[33] Y. Kuroda, A. Kawashima, Y. Hayashi, H. Ogoshi, J. Am. Chem. Soc. 119 (1997) 4929.
[34] R.P. Bonar-Law, J.K.M. Sanders, J. Am. Chem. Soc. 117 (1995) 259.
[35] I. Tabushi, S-I Kugimmiya, M.G. Kinnaird, T. Sasaki, J. Am. Chem. Soc. 107 (1985) 4129.
[36] Y. Aoyama, A. Yamagishi, M. Asagawa, H. Toi, H. Ogoshi, J. Am. Chem. Soc. 110 (1988) 4076.
[37] Y. Aoyama, M. Asakawa, A. Yamagishi, H. Toi, H. Ogoshi, J. Am. Chem. Soc. 112 (1990) 3145.

[38] T. Mizutani, T. Ema, T. Tomita, Y. Kuroda, H. Ogoshi, J. Am. Chem. Soc. 116 (1994) 4240.
[39] T. Mizutani, T. Ema, H. Ogoshi, Tetrahedron 51 (1995) 473.
[40] T. Mizutani, T. Murakami, H. Ogoshi, Tetrahedron Lett. 37 (1996) 5369.
[41] A.W. Maverick, M.L. Ivie, J.H. Waggenspack, F.R. Fronczek, Inorg. Chem. 29 (1990) 2403.
[42] M.S. Goodman, J. Weiss, A.D. Hamilton, Tetrahedron Lett. 35 (1994) 8943.
[43] M.S. Goodman, A.D. Hamilton, J. Weiss, J. Am. Chem. Soc. 117 (1995) 8447.
[44] H. Ogoshi, H. Hatakeyama, J. Kotani, A. Kawashima, Y. Kuroda, J. Am. Chem. Soc. 113 (1991) 8181.
[45] T. Hayashi, T. Miyahara, N. Hashizume, H. Ogoshi, J. Am. Chem. Soc. 115 (1993) 2049.
[46] C.K. Chang, Y. Liang, G. Aviles, J. Am. Chem. Soc. 117 (1995) 4191.
[47] Y. Ling, C.K. Chang, Tetrahedron Lett. 36 (1995) 3817.
[48] M. Yamamoto, M. Takeuchi, S. Shinkai, Tetrahedron 54 (1998) 3125.
[49] T. Mizutani, T. Ema, T. Yoshida, Y. Kuroda, H. Ogoshi, Inorg. Chem. 32 (1993) 2072.
[50] T. Mizutani, T. Ema, T. Yoshida, T. Renne, H. Ogoshi, Inorg. Chem. 33 (1994) 3558.
[51] T. Imada, H. Kijima, M. Takeuchi, S. Shinkai, Tetrahedron 52 (1996) 2817.
[52] T. Mizutani, T. Kurahashi, T. Murakami, N. matsumi, H. Ogoshi, J. Am. Chem. Soc. 119 (1997) 8991.
[53] M. Takeuchi, H. Kijima, I. Hamachi, S. Shinkai, Bull. Chem. Soc. Jpn. 70 (1997) 699.
[54] S. Arimori, M. Takeuchi, S. Shinkai, Chem. Lett. (1996) 77.
[55] M. Takeuchi, T. Imada, S. Shikai, Bull. Chem. Soc. Jpn. 71 (1998) 1117.
[56] M.J. Crossley, L.G. Mackay, A.C. Try, J. Chem. Soc. Chem. Commun. (1995) 1925.
[57] T. Hayashi, M. Nonoguchi, T. Aya, H. Ogoshi, Tetrahedron Lett. 38 (1997) 1603.
[58] T. Ema, S. Misawa, S. Nemugaki, T. Sakai, M. Utaka, Chem. Lett. (1997) 487.
[59] Y. Kuroda, Y. Kato, T. Higashioji, H. Ogoshi, Angew. Chem. Int. Ed. Engl. 32 (1993) 723.
[60] Y. Kuroda, Y. Kato, T. Higashioji, J-y. Hasegawa, S. Kawanami, M. Takahashi, N. Shiraishi, K. Tanabe, H. Ogoshi, J. Am. Chem. Soc. 117 (1995) 10950.
[61] R. Cacciapaglia, S. Di Stefano, E. Kelderman, L. Mandolini, Angew. Chem. Int. Ed. Engl. 38 (1999) 348.
[62] W. Zhang, J.L. Loebach, S.R. Wilson, E.N. Jacobsen, J. Am. Chem. Soc. 112 (1990) 2801.
[63] R. Irie, K. Noda, Y. Ito, N. Matsumota, T. Katsuki, Tetrahedron Lett. 31 (1990) 7345.
[64] C.F. Martens, R.J.M. Klein Gebbink, M.C. Feiters, R.J.M. Nolte, J. Am. Chem. Soc. 116 (1994) 5667.
[65] J.T. Groves, T.E. Nemo, J. Am. Chem. Soc. 105 (1983) 5786.
[66] J.T. Groves, R.S. Myers, J. Am. Chem. Soc. 105 (1983) 5791.
[67] S. O'Malley, T. Kodadek, Tetrahedron Lett. 32 (1991) 2445.
[68] Y. Naruta, F. Tani, K. Maruyama, Chem. Lett. (1989) 1269.
[69] R. Zhang, W-Y. Yu, T-S. Lai, C-M. Che, Chem. Commun. (1999) 409.
[70] K. Ohkubo, T. Sagawa, M. Kuwata, T. Hata, H. Ishida, J. Chem. Soc. Chem. Commun. (1989) 352.
[71] S. Vlain, P. Maillard, M. Momenteau, J. Chem. Soc. Chem. Commun. (1994) 1697.
[72] K. Konishi, K. Oda, K. Nishida, T. Aida, S Inoue, J. Am. Chem. Soc. 114 (1992) 1313.
[73] L. Weber, I. Imiolczyk, G. Haufe, D. Rehorek, H. Hennig, J. Chem. Soc. Chem. Commun. (1992) 301.
[74] J.P. Collman, Z. Wang, A. Straumanis, M. Quelquejeu, J. Am. Chem. Soc. 121 (1999) 460.
[75] H. Furuta, M.J. Cyr, J.L. Sessler, J. Am. Chem. Soc. 113 (1991) 6677.
[76] K. Eshima, Y. Matsushita, E. Haegawa, H. Nishide, E. Tsuchida, Chem. Lett. (1989) 381.
[77] G. Blondeel, A. Harriman, G. Porter, A. Wilowska, J. Chem. Soc. Faraday Trans. 2 (1984) 867.
[78] J. Monod, J.P. Changeux, F. Jacob, J. Mol. Biol. 6 (1963) 306.
[79] M.F. Perutz, Annu. Rev. Biochem. 48 (1979) 327.
[80] N. Shibayama, S. Saigo, J. Am. Chem. Soc. 121 (1999) 444.
[81] P.R. Sijbesma, R.J.M. Nolte, J. Am. Chem. Soc. 113 (1991) 6695.
[82] J. Rebek Jr., T. Costello, L. Marshall, R. Wattley, R.C. Gadwood, K. Onan, J. Am. Chem. Soc. 107 (1985) 7481.
[83] H.-J. Schneider, D. Ruf, Angew. Chem. Int. Ed. Engl. 29 (1990) 1159.

[84] W.O. McClure, G.M. Edelman, Biochemistry 5 (1966) 1908.
[85] K.L. Cole, M.A. Farran, K. Deshayes, Tetrahedron Lett. 33 (1992) 599.
[86] R. Baldes, H.-J. Schneider, Angew. Chem. Int. Ed. Engl. 34 (1995) 321.
[87] G. Deng, T.D. James, S. Shinkai, J. Am. Chem. Soc. 116 (1994) 4567.
[88] T.D. James, S. Shinkai, J. Chem. Soc. Chem. Commun. (1995) 1483.
[89] F. Ohseto, H. Yamamoto, H. Matsumoto, S. Shinkai, Tetrahedron Lett. 36 (1995) 6911.
[90] H. Murakami, S. Shinkai, Tetrahedron Lett. 34 (1993) 4237.
[91] S. Shinkai, K. Iwamoto, K. Araki, T. Harada, T. Matsuda, Chem. Lett. (1990) 1263.
[92] K. Iwamoto, A. Ikeda, K. Araki, T. Harada, S. Shinkai, Tetrahedron 49 (1993) 9937.
[93] U. Knof, A. von Zelewsky, Angew. Chem. Int. Ed. Engl. 38 (1999) 302.
[94] T. Mizuno, M. Takeuchi, I. Hamachi, K. Nakashima, S. Shinkai, J. Chem. Soc. Perkin. Trans. 2 (1998) 2281.
[95] M. Yamamoto, M. Takeuchi, S. Shinkai, Tetrahedron Lett. 39 (1998) 1189.